

## **Ceramide induces a loss of cytosolic peroxide in mononuclear cells.**

<sup>1,2</sup>Darren C. Phillips and <sup>1</sup>Helen R. Griffiths

Running Title – Ceramide reduces cytosolic peroxide.

<sup>1</sup>Molecular Biosciences Group,

Life and Health Sciences,

Aston University,

Aston Triangle,

Birmingham B4 7ET, UK

Tel: +044 (0)121 359 3611 Ext. 5226

Fax: +044 (0)121 359 5142

Email: [h.r.griffiths@aston.ac.uk](mailto:h.r.griffiths@aston.ac.uk)

<sup>2</sup>Present Address

Division of Molecular Therapeutics,

Department of Hematology-Oncology,

St Jude Children's Research Hospital

DT 5062

332 North Lauderdale

Memphis, TN 38105, USA

\*

---

**\* Abbreviations.**

A-SMase, acid sphingomyelinase; BSA, bovine serum albumin; CD-95L, CD-95 ligand; DAG, diacylglycerol; C<sub>2</sub>-ceramide, N-acetyl-sphingosine; C<sub>6</sub>-ceramide, N-hexanoyl-sphingosine; DAGK, diacylglycerol kinase; DCF, 2', 7'-dichlorofluorescein; DCFH, non-fluorescent 2', 7'-dichlorofluorescein; DCFH-DA, 2', 7'-dichlorofluorescein diacetate; DMSO, dimethyl sulfoxide; FS, forward scatter; GSH, glutathione; GSSG, oxidised glutathione; MdX, median X; NAC, N-acetyl cysteine; N-SMase, neutral sphingomyelinase; PBL, peripheral blood lymphocyte; PBMNC, peripheral blood mononuclear cells; PBS, phosphate buffered saline; PHA, phytohemagglutinin; PI, propidium iodide; ROS, reactive oxygen species; SMase, sphingomyelinase; SOD, superoxide dismutase; SS, side scatter; TLC, thin layer chromatography; TNF $\alpha$ , tumour necrosis factor alpha; [peroxide]<sub>cyt</sub>, cytosolic peroxide; [peroxide]<sub>m</sub>, mitochondrial peroxide;  $\Delta$ DCF, change in DCF.

## Synopsis.

Ceramide (a sphingolipid) and reactive oxygen species (ROS) are each partly responsible for intracellular signal transduction in response to a variety of agents. It has been reported that ceramide and ROS are intimately linked, and show reciprocal regulation. Utilising synthetic, short chain ceramide to mimic the cellular responses to fluctuations in natural endogenous ceramide formation, or stimulation of CD95 to induce ceramide formation, we describe that the principal redox altering property of ceramide is to lower the cytosolic peroxide concentration. Apoptosis of Jurkat T-cells, primary resting and PHA activated human peripheral blood T lymphocytes was preceded by loss in cytosolic peroxide ( $[\text{peroxide}]_{\text{cyt}}$ ), measured by the peroxide sensitive probe DCFH-DA (also reflected in a lower rate of SOD inhibitable cytochrome c reduction), and this was not associated with loss of membrane integrity. Where growth arrest of U937 monocytes was observed with no loss of membrane integrity, the reduction in cytosolic peroxide was of a lower magnitude than that preceding the onset of apoptosis in T-cells. Furthermore, reducing the cytosolic peroxide level in U937 monocytes prior to the application of synthetic ceramide by pre-treatment with either of the anti-oxidants N-acetyl cysteine (NAC) or glutathione (GSH) conferred apoptosis. However, NAC or GSH did not affect the kinetics or magnitude of ceramide induced Jurkat T-cell apoptosis. Therefore, the primary redox effect of cellular ceramide accumulation is to lower the  $[\text{peroxide}]_{\text{cyt}}$  of both primary and immortalised cells, the magnitude of which dictates the cellular response.

**Keywords:** apoptosis, growth arrest, CD95, reactive oxygen species, redox compartmentalisation.

## Introduction.

The sphingolipid ceramide has been identified as an important, but not exclusive, signalling intermediate in the induction of cellular responses to a variety of agents. These include both physiological, e.g. TNF $\alpha$  [1-4], interleukin-1 $\beta$  [IL-1 $\beta$ ; 5], CD-95 (APO-1/Fas; 1,6-8] and toxicological, e.g. hydrogen peroxide (H<sub>2</sub>O<sub>2</sub>), heat shock, UV light, ionising radiation [4, 9], anticancer drugs [10-12] or the bacterial endotoxin LPS [13]. Ceramide accumulation in response to extracellular agents appears to be driven either by the action of sphingomyelinases (SMase), catalysing the hydrolysis of sphingomyelin to ceramide [2, 6, 9], or through *de novo* ceramide generation via ceramide synthase [10-11]. Downstream events, which vary according to cell type and stimulus, include apoptosis and proliferation, following activation of intracellular signalling cascades.

The application of cell permeable, synthetic ceramides or bacterial sphingomyelinase to a variety of cell types is able to induce the apoptotic [2, 4, 12] and proliferative [14] responses supporting a cell type specific signalling role. Cell cycle arrest by dephosphorylation of the retinoblastoma gene product [13,15,16], differentiation [17], and senescence [18] have also been observed upon cell treatment with synthetic ceramide.

Endogenous cellular ceramide and ROS levels are elevated in response to overlapping external stimuli, and the external application of synthetic ceramides or the ROS, H<sub>2</sub>O<sub>2</sub>, induces the activation of common downstream protein targets. Therefore, evidence suggests that the effects of ROS and ceramide are intimately related. Indeed, recent observations are suggestive of an association between ROS and ceramide at two levels; firstly, in regulation of ceramide metabolism where the intracellular antioxidant negatively regulates the activity of neutral sphingomyelinase (N-SMase) but not acid sphingomyelinase [A-SMase; 2, 19, 20], and secondly as a putative mediator of ceramide signalling following disruption of the mitochondrial electron transport chain [21-24].

However, the effects of antioxidants in detoxifying ceramide-induced apoptosis are inconsistent. U937 monocytes or MCF-7 breast carcinoma cell lines are not protected from short chain ceramide induced cell death by pre-treatment with the antioxidants GSH and NAC [2, 25] whereas catalase was reported to antagonise the lethality of C<sub>2</sub>-ceramide in WEHI 231 B cells [26]. Additionally, in U937 monocytes, C<sub>2</sub>-ceramide did not lead to the predicted enhancement of fluorescence by the cytosolic peroxide sensitive dye DCF [25].

We have previously described that the cellular responses of apoptosis or growth arrest induced by synthetic ceramides are associated with the degree of magnitude of [peroxide]<sub>m</sub> formation and the associated alteration in redox state [23]. However, we also observed that BSO-mediated GSH depletion in monocytes and T cells protected against ceramide induced changes in cell cycle, indicating that complex compartmental differences in levels of oxidants/antioxidants may govern outcome. Furthermore, given the relatively small perturbation in [peroxide]<sub>m</sub> observed we questioned whether these changes are capable of promoting extra-mitochondrial signalling. Consequently, we have investigated the effects of ceramide, and its generation by the physiological CD95 ligand (CD95L), on the cytosolic peroxide concentration ([peroxide]<sub>cyt</sub>) in the context of the ensuing cellular response. Herein, we describe that the primary redox effect of cellular ceramide accumulation is to lower the [peroxide]<sub>cyt</sub> of both primary and immortalised cells, the magnitude of which dictates the cellular response.

## Experimental

### *Materials.*

All reagents were obtained from Sigma Chemical Company (Poole, UK), solvents were from Fisher (Loughborough, UK) and all gases from BOC Ltd (Guildford, UK) unless otherwise stated. RPMI 1640, foetal bovine serum and penicillin (1000U/ml)/streptomycin (10,000µg/ml; P/S) were purchased from GibcoBRL (Paisley, UK). Human monoclonal anti-human CD95 (Fas/APO-1) antibody was from R&D Systems (Abingdon, UK). C<sub>2</sub>-ceramide (N-acetyl-sphingosine) and C<sub>6</sub>-ceramide (N-hexanoyl-sphingosine), were obtained from Biomol Research Laboratories (Plymouth Meeting, PA, USA). *Escherichia coli* diacylglycerol kinase (DAGK) and n-octyl-β-D-glycopyranoside were purchased from Calbiochem (Nottingham, UK). [<sup>32</sup>P] ATP was purchased from Amersham Life Science Ltd. (Little Charford, UK). Fluorescently tagged monoclonal antibodies (MoAb) and isotype negative controls were obtained from Diaclone, (Besançon Cedex, France) or Serotec Ltd (Kidlington, UK).

2', 7',-dichlorofluorescein diacetate (DCFH-DA) was dissolved in dimethyl sulfoxide (DMSO) to stock solutions of 75mM. Subsequent dilutions were made with serum free RPMI 1640. The antioxidants N-acetylcysteine (NAC) and glutathione (GSH) were made up in serum free RPMI 1640. In the [peroxide]<sub>cyt</sub> assays, the final cellular concentration of DMSO employed did not exceed 0.1%. Monoclonal anti-human CD95 (Fas/APO-1) antibody was reconstituted in sterile phosphate buffered saline (PBS; 0.01M Na<sub>2</sub>HPO<sub>4</sub>, 0.002M KH<sub>2</sub>PO<sub>4</sub>, 0.003M KCl, 0.137M NaCl; pH 7.4) containing 0.1% fraction V bovine serum albumin to a concentration of 500µg/ml with further dilutions being made in PBS/0.1% BSA. C<sub>2</sub>-/C<sub>6</sub>-ceramide were dissolved in anhydrous DMSO to a stock solution of 20mM. Subsequent dilutions were made in 1mM fatty acid free BSA in PBS.

## *Methods*

### *Cell culture and stimulation.*

The acute human T-cell leukaemia cell line, Jurkat, and the human monocyte cell line, U937, were maintained in RPMI 1640 media, supplemented with 10% heat inactivated foetal calf serum and 1% penicillin/streptomycin. Cells were incubated at 37°C in a humidified atmosphere of 5% CO<sub>2</sub> and 95% air. The number of viable cells per ml was determined by trypan blue exclusion using an improved Neubauer haemocytometer (Weber Scientific International Ltd., Teddington, UK). Cells at a concentration of 2x10<sup>6</sup>/ml were serum starved for 4 hours in the described incubator conditions prior to treatment. Where indicated, cells were treated with CD95L or C<sub>2</sub>-/C<sub>6</sub>-ceramide for the times and concentrations noted, incubations at 37°C in a humidified 5% CO<sub>2</sub>/95% air incubator. To investigate the role of reactive oxygen species (ROS) in the cellular responses to the above agents, cell suspensions were pre-treated for 4 hours with 10mM NAC or GSH. The role of surface gamma glutamyl transpeptidase activity in providing the GSH-mediated antioxidant protection was investigated through pre-incubation of cells with 1mM acivicin for 30 minutes prior to GSH exposure. To prevent the cellular export of glutathione disulphide (GSSG), cells were pre-treated for 1 hour with L-methionine or L-cystathionine [34]. Further inhibitory experiments with the NADPH oxidase inhibitor, diphenylene iodonium (2.5µM), were established in order to elucidate any role of this enzyme in modulation of intracellular redox. Stimulation was discontinued by removing cells suspensions from culture vessels, centrifuging at 1000xg (Eppendorf centrifuge 5415D, Hamburg, Germany) for 5 minutes and washing twice with 1ml of ice cold PBS prior to further experimental manipulation.

Individual additions to cells suspensions did not exceed 1% of the total volume and were dispersed with gentle mixing by pipette. Control experiments were conducted under identical conditions as tests, employing vehicle treatment.

*T-cell isolation and cell culture.*

Briefly, 40mls of venous blood was obtained from consenting adults into 10% sodium citrate (4% w/v) to prevent coagulation. Further manipulation of the blood was conducted under aseptic conditions. Blood was diluted with PBS containing 0.1% BSA (w/v) in the ratio 2:5 into 50ml conical tubes (Orange Scientific, Braine-l'Alleud, Belgium). Peripheral blood mononuclear cells (PBMNC) were isolated by density gradient centrifugation over Lymphoprep<sup>TM</sup> (Nycomed Pharma AS, Oslo, Norway) and the resting T-cells purified by negative isolation employing magnetic beads (Dynal A.S., Oslo, Norway). For *ex vivo* examination, T-cells were analysed for [peroxide]<sub>cyt</sub> and lipid content immediately following isolation. Additionally, resting T-cells were cultured for 72 hours in RPMI 1640 supplemented with 10% FCS and 1% penicillin/streptomycin (P/S) with or without 10 $\mu$ g of phytohemagglutinin (PHA) per 2x10<sup>6</sup> /ml T-cells to elicit activation. Isolated T-cells were incubated at 37°C in a humidified atmosphere of 5% CO<sub>2</sub> and 95% air. Prior to further experimental manipulation, T-cells in culture were washed twice, resuspended in serum free RPMI 1640 and treated as described for immortalised cell lines

*Phenotypic analysis of peripheral blood lymphocytes by immunofluorescence.*

The percentage of CD3<sup>+</sup> peripheral blood T-lymphocytes (PBL) and their percentage activation (determined as the appearance of CD25 (IL-2 $\alpha$  receptor) was evaluated by flow cytometry following negative isolation from blood. The purity of extracted PBL was assessed by the percentage of CD3<sup>+</sup> PBL and monocyte contamination evaluated by the presence of CD14<sup>+</sup> cells within the whole sample. PBS washed PBL *ex vivo* or following 72 hour culture were treated with 10 $\mu$ l of antibody per 10<sup>6</sup> cells and incubated on ice in the dark for 30 minutes. The antibodies used were the mouse monoclonal anti-human CD3 antigen (PE conjugated), mouse monoclonal anti-human CD25 antigen (FITC conjugated) and mouse monoclonal anti-human CD14 antigen (RPE-Cy5 conjugated). For each sample,

isotype negative controls of the MoAb were used to establish background fluorescence. PBL were fixed in 250µl of 4% formaldehyde solution. Samples were then vortexed vigorously and incubated in the dark for a further 15 minutes followed by the addition of 200µl of Isoton (Beckman Coulter, Miami, FL, USA). Samples were again vortexed and incubated in the dark, at room temperature for a minimum of 10 minutes. Samples were stored in the dark at 4°C for up to 24 hours prior to analysis without significantly affecting results. Samples were then analysed by flow cytometry (EPICS® XL-MCL, Beckman Coulter) utilising 3-way colour compensation and corrected for background fluorescence detected with isotype negative controls. A minimum of 10,000 PBL were analysed per sample using the following gating strategy: The percentage activation of CD3<sup>+</sup> PBL was evaluated on a dual parameter histogram of log FL2 (CD3 PE) versus log FL1 (CD25 FITC). The purity of PBL extracted was assessed as the percentage of CD3<sup>+</sup> cells on an ungated histogram of side scatter (SS) versus log FL2 (CD3 PE). Monocyte contamination was determined on an ungated histogram of log FL4 (CD14 PE-Cy5) versus count.

*Flow cytometric DNA cell cycle analysis.*

Briefly, PBS washed cells were centrifuged at 100xg (Eppendorf centrifuge 5415D, Hamburg, Germany) for 5 minutes, the supernatant removed and the resulting cell pellet resuspended in 1ml hypotonic fluorochrome solution (50µg/ml PI in 0.1% sodium citrate and 0.1% Triton x-100) to extract and stain nucleoids [27]. Samples were incubated in the dark at 4°C for 14-24 hours prior to flow cytometric cell cycle analysis. Propidium iodide (PI) fluorescence of individual nuclei was measured using an EPICS® XL-MCL flow cytometer (Beckman-Coulter) equipped with a 488nm air-cooled Argon laser. Forward scatter (FS) and SS of the nuclei were simultaneously measured in addition to linear and log red fluorescence (FL3, bandwidth 605nm-635nm). Clumps of nuclei were eliminated by appropriate gating. For each analysis, 20,000 events were recorded on the gated FL3 detector. The percentage of

actual apoptosis was determined by quantifying the number of hypoploid (subdiploid) nuclei. Values were also expressed as a percentage of specific apoptosis according to the formula  $\text{specific apoptosis} = (T-C)/(100-C) \times 100$ , where T equals the percentage of apoptotic events from treated cells, and C equals the percentage of apoptotic events from control cells. The percentage of nuclei in the G0/G1 phase of the cell cycle was quantified using Multi-Cycle for Windows (Phoenix Flow Systems, San Diego, U.S.A.).

*Evaluation of cytosolic peroxide levels.*

A procedure adapted from Bass *et al.*, [28] was used to measure cytosolic peroxide levels ( $[\text{peroxide}]_{\text{cyt}}$ ) cells by flow cytometry as the fluorescence generated from cells loaded with the peroxide sensitive fluorescent probe DCFH-DA. DCFH-DA rapidly diffuses into the cytosol of cells where it is hydrolysed to the non-fluorescent, oxidation sensitive DCFH. In the presence of  $[\text{peroxide}]_{\text{cyt}}$ , DCFH is rapidly oxidised to the non-diffusible, fluorescent DCF. Cells were loaded with 50 $\mu\text{M}$  DCFH-DA per  $2 \times 10^6$  cells for the final 40 minutes of exposure to varying concentrations and incubation periods with CD95 or ceramide. Immediately following agent/DCFDA incubation, cells were analysed by flow cytometry (EPICS<sup>®</sup> XL-MCL), with the first control population always adjusted to the third log decade, giving a Mdx value of  $\sim 100$ . Measurements of FS, side SS and log FL1 fluorescence (green light, band width 505nm-545nm) were recorded. The viable cell population, determined by FS and SS properties, were gated to exclude debris, clumped cells or machine noise. 10,000 cells were examined from each sample on a histogram of log FL1 (DCF fluorescence) versus count. In control experiments, DCF was seen to have no quenching effect on hydrogen peroxide induced DCF fluorescence.

*Evaluation of SOD-inhibitable cytochrome c reduction.*

Cells (200 $\mu\text{l}$  of  $10^7/\text{ml}$ ) in HBSS, were dispensed into a optically clear flat bottomed 96 well plate containing 160 $\mu\text{M}$  cytochrome c, in the presence or absence of C<sub>2</sub>- ceramide

(20 $\mu$ M) and either superoxide dismutase (3000U/ml) or diphenylene iodonium (2.5 $\mu$ M). Cytochrome c reduction was monitored at 550nm following incubation with the aforementioned agents at 37°C for 1 hour or 16 hours. Superoxide release was calculated in nmols/ $10^7$  cells using the molar extinction coefficient for cytochrome c as  $21 \times 10^3 \text{ M}^{-1} \text{ cm}^{-1}$  at an 550nm.

*Analysis of [peroxide]<sub>cyt</sub> levels of mononuclear cells from peripheral whole blood.*

Blood (200 $\mu$ l) was treated with C<sub>2</sub>-/C<sub>6</sub>-ceramide, for 1 hour in a water bath in the dark at 37°C with gentle horizontal shaking. Optimal concentrations were pre-determined from the responses achieved from cell lines *in vitro*. At T<sub>end</sub> -20 minutes, DCFH-DA was added to give a final concentration of 50 $\mu$ M, and samples returned to the water bath. At the end of agent treatment period, blood was stained with antibodies at a saturating concentration of at least 10 $\mu$ l of antibody per 100 $\mu$ l of blood. Samples were then incubated on ice for a further 30 minutes. To identify monocytes and T-cells, PBL were stained with mouse monoclonal anti-human CD3 antigen PE conjugated and mouse monoclonal anti-human CD14 RPE-Cy5 conjugated respectively. 3-way colour compensation to account for overlapping emission spectra of the fluorescent-tagged antibodies and DCF was applied. Red blood cells were lysed and the mononuclear cell (MNC) population fixed with Optilyse C (Beckman Coulter), as described above. Cell suspensions were immediately analysed by flow cytometry. Histograms of log FL2 (CD3 PE) versus SS and log FL4 (CD14 RPE-Cy5) versus SS were used to gate CD3<sup>+</sup> lymphocytes and CD14<sup>+</sup> monocytes respectively. The DCF fluorescence of CD3<sup>+</sup> T-lymphocytes and CD14<sup>+</sup> monocytes were analysed on separate single parameter histograms of log integral FL1 (DCF) versus count. The median fluorescence (MdX) intensity of each sample was recorded.

*Determination of intracellular glutathione content*

This was done according to the recycling assay of Tietze, [29]. Briefly, at the end of each treatment period, samples were washed with ice cold PBS by centrifugation at 2,300rpm for 5 minutes. An aliquot was removed for protein determination and then cells were resuspended in 3.33% 5-sulfosalicylic acid dihydrate, vortexed vigorously and centrifuged at 13,000rpm to precipitate interfering proteins. Supernatant (25 $\mu$ l) was added to 50 $\mu$ l 5,5'-Dithio-bis (2-Nitrobenzoic acid; DTNB; 6mM), and 150 $\mu$ l NADPH (0.3mg/ml) in triplicate, and incubated at 37°C for 3 minutes, prior to addition of 25 $\mu$ l glutathione reductase (GSR; 20U/ml). The plate was immediately read at 420nm and then read again at +1 and +5 minutes to determine DTNB reduction. Test sample values were calibrated against a standard curve of glutathione from 0-60nmoles, and expressed per mg of cellular protein.

#### *Protein Determination*

Protein concentration was determined in quadruplicate using the BCA assay based on the method of Smith *et al.*, [30], using bovine serum albumin (BSA) as standards to calculate unknowns.

#### *Quantification of endogenous T-cell ceramide content.*

Lipids were extracted from Jurkat T-cells (2x10<sup>6</sup>/ml) according to the method of Bligh & Dyer, [31] and the concentration of ceramide quantified by the DAGK assay as described [32, 33]. The mass of ceramide and DAG extracted from each cell sample was obtained from the standard curve constructed from known concentrations of type III ceramide (from bovine brain; Sigma, Poole, UK) and standardised as the lipid concentration per 10<sup>6</sup> cells. The efficiency of the assay was evaluated from the standard curve and a known concentration of C<sub>6</sub>-ceramide. Cellular ceramide levels were adjusted according to the % efficiency of conversion and were always greater than 90%.

#### *Statistical analysis.*

Statistical analysis was performed by one-way ANOVA followed by Tukey's or Dunnet's post *hoc* test analysis, or Student's *t*-test. A  $p < 0.05$ ,  $p < 0.01$  or  $p < 0.001$  was considered to be significant.

## Results.

As previously reported [23], the treatment of Jurkat T-cells with 20 $\mu$ M C<sub>2</sub>-/C<sub>6</sub>-ceramide induced a rapid, time dependent elevation in the percentage of specific apoptosis which was significant at 3hours, but was not observed at the lower synthetic ceramide concentration of 1-10 $\mu$ M (see Figure 1a). Maximal specific apoptosis (55%) was observed following 8hrs treatment with 20 $\mu$ M C<sub>2</sub>-ceramide. Treatment of Jurkat T-cells for longer periods of up to 36 hours with 20 $\mu$ M C<sub>2</sub> -ceramide did not further increase the percentage of specific apoptosis ( $p>0.05$ ; see Figure 1a). Comparable kinetics of apoptosis in Jurkat T-cells were observed with 0-20 $\mu$ M C<sub>6</sub>-ceramide (data not shown) [23].

During the first 16 hours of Jurkat T-cell exposure to C<sub>2</sub>-ceramide, [peroxide]<sub>cyt</sub> was monitored by flow cytometry using the fluorescence emission of DCF from cells pre-loaded with the peroxide sensitive dye DCFH-DA. The median fluorescence (Mdx) of the DCFH-DA treated viable cell population, determined by FS and SS properties, decreased with immediately following exposure to 20 $\mu$ M C<sub>2</sub>-ceramide. The first significant decreases in DCF Mdx were observed at 15 minutes exposure to 20 $\mu$ M C<sub>2</sub>-ceramide ( $p<0.05$ ) when compared to vehicle treated control Jurkat T cells. Basal peroxide levels were fixed to  $\sim$ Mdx=100, where a maximum decrease in  $\Delta$ DCF Mdx of approximately -60 arbitrary units (a.u) was observed at 4 hours treatment with 20 $\mu$ M C<sub>2</sub>-ceramide (see Figure 1b). DCF fluorescence of cells exposed to 20 $\mu$ M C<sub>2</sub>-ceramide for greater than 8 hours was not measured as no further alteration in specific apoptosis were observed at these longer incubation periods.  $\Delta$ DCF Mdx induced by 16 hours treatment of Jurkat T cells with 10 $\mu$ M C<sub>2</sub>-ceramide fell significantly to approximately -35 a.u ( $p<0.01$ ) (see Figure 1b) without the appearance of apoptosis ( $p>0.05$ ; see Figures 1a & b). Similar alterations in  $\Delta$ DCF Mdx of Jurkat T-cells treated with 20 $\mu$ M C<sub>2</sub>-ceramide were observed after 45 minutes (see Figure 1b)

and this was not associated with the appearance of apoptosis at this time point ( $p>0.05$ ; see Figures 1a). Similar effects on the DCF fluorescence were observed in Jurkat T-cells following treatment with 0-20 $\mu$ M C<sub>6</sub>-ceramide (data not shown).

As previously reported by us [23] treatment of the human monocytic cell line U937 with either C<sub>2</sub>- or C<sub>6</sub>-ceramide (0-20 $\mu$ M) for up to 36 hours induced an enhancement in the percentage of nuclei in the G<sub>0</sub>/G<sub>1</sub> phase of the cell cycle when compared to vehicle treated controls, first evident following 16 hrs treatment of U937 cells with 20 $\mu$ M C<sub>2</sub>-/C<sub>6</sub>-ceramide ( $p<0.05$ ; data not shown). This was also observed at longer incubation periods with 10 $\mu$ M C<sub>6</sub> ceramide ( $p<0.05$ ; see Figure 2a). The elevation in U937 monocyte nucleoids in the G<sub>0</sub>/G<sub>1</sub> phase of the cell cycle was associated with the prevention of apoptosis induced by serum withdrawal. Low dose C<sub>6</sub>-ceramide (1 $\mu$ M) exposure for 36 hours did not significantly affect either the percentage of nucleoids in the G<sub>0</sub>/G<sub>1</sub> phase of the cell cycle ( $p>0.05$ ) nor the percentage of actual apoptosis compared to that observed in vehicle treated control U937 monocytes ( $p>0.05$ ; see Figure 2a). Monocytes treated with either 10 or 20 $\mu$ M C<sub>6</sub>-ceramide for 36 hours showed significantly elevated G<sub>0</sub>/G<sub>1</sub> DNA content compared to vehicle controls ( $p<0.01$ ). At 36 hours, the G<sub>0</sub>/G<sub>1</sub> content remained elevated to of the same extent as U937 monocytes treated with 10 or 20 $\mu$ M C<sub>6</sub>-ceramide for 24 hours (data not shown;  $p<0.05$ ). Correspondingly, the synthetic ceramide treatment of U937 monocytes induced a dose dependent inhibition of serum deprivation induced actual apoptosis. C<sub>6</sub>-ceramide (10 $\mu$ M) treatment for 36 hours significantly inhibited the appearance of actual apoptosis due to serum starvation by approximately 12% ( $p<0.05$ ). Greater protection against actual apoptosis by 18% ( $p<0.01$ ) was seen following 20 $\mu$ M C<sub>6</sub>-ceramide (see Figure 2a). Identical results were obtained following treatment of U937 monocytes with C<sub>2</sub>-ceramide (Data not shown).

In U937 cells, no alteration in the intracellular H<sub>2</sub>O<sub>2</sub> concentration (as DCF fluorescence) was observed for the first 30 minutes of 20 $\mu$ M C<sub>6</sub>-ceramide exposure when

compared to vehicle treated control cells (see Figure 2b).  $\Delta$ DCF MdX then rapidly decreased to a minimum of -40 in C<sub>6</sub>-ceramide treated U937 cells respectively within 4hrs, which then rose to -25 a.u. on increasing the treatment period to 8 hours (see Figure 2b).  $\Delta$ DCF MdX remained at -25 a.u. at 16 hours incubation with 20 $\mu$ M C<sub>6</sub>-ceramide. At a lower concentration (10 $\mu$ M), C<sub>6</sub>-ceramide decreased DCF fluorescence compared to control with slower kinetics than that observed with the higher dose (20 $\mu$ M), and with less potency at all time points examined (2, 4 and 16 hours,  $p < 0.05$ ; see Figure 2b). The maximal decreases in  $\Delta$ DCF MdX of U937 cells monocytes treated with 20 $\mu$ M ceramide were significantly less than those achieved in Jurkat T-cells ( $p < 0.01$ ; Figures 1b & 2 b).

Flow cytometric evaluation of the cellular uptake of the membrane impermeable dye PI and cell size revealed no evidence of necrosis in U937 monocytes treated with C<sub>2</sub>-/C<sub>6</sub>-ceramide (0-20 $\mu$ M) for up to 16 hours. This was confirmed in Jurkat T-cells treated with 0-10 $\mu$ M C<sub>2</sub>-/C<sub>6</sub>-ceramide for 16 hours and 20 $\mu$ M C<sub>2</sub>-/C<sub>6</sub>-ceramide for up to 8 hours. However, following 16 hours treatment of Jurkat T-cells with 20 $\mu$ M C<sub>2</sub>-/C<sub>6</sub>-ceramide, a subpopulation of Jurkat T-cells possessed reduced cell size with high PI uptake indicating late apoptosis or secondary necrosis (data not shown). To confirm the specificity of effect on DCF fluorescence, ceramide metabolite, sphingosine-1-phosphate (S1P), was also examined. S1P had no effect on DCF fluorescence (data not shown).

In order to establish the contribution of NADPH oxidase activity to any change in [peroxide]<sub>cyt</sub> that was measured as  $\Delta$ DCF MdX, we treated cells with the NADPH oxidase inhibitor diphenylene iodonium (DPI), and analysed for ceramide induced changes in DCF fluorescence and apoptosis. After one hour, DPI alone or in combination with 20 $\mu$ M C<sub>2</sub>-ceramide did not significantly alter the DCF fluorescence observed in either Jurkat T-cells or U937 monocytes exposed to 20 $\mu$ M C<sub>2</sub>-ceramide alone (data not shown). By 16 hours, DPI significantly reduced DCF MdX in U937 cells, with a trend to further reduction when co-

incubated with ceramide (see Figure 3a). Indeed examination of the effects of DPI on apoptosis showed that while inducing slight apoptosis on its own ( $7.8 \pm 0.9\%$ ), co-incubation with C<sub>2</sub>-ceramide significantly enhanced apoptosis in U937 cells to  $18.6 \pm 2.3\%$  ( $p < 0.001$ ) compared with C<sub>2</sub>-ceramide alone (see Figure 3c). In addition, DPI significantly promoted C<sub>2</sub>-ceramide-induced apoptosis in Jurkat T cells ( $p < 0.001$ ; see Figure 3d). Figure 3b shows that this was associated with a significant reduction in DCF MdX (16 hours: ceramide alone = 72 a.u., ceramide + DPI = 25.7 a.u.;  $p < 0.001$ ).

As an alteration in DCF fluorescence may be a representation of changing availability of catalyst or hydrolysis of DCFH-DA in ceramide treated cells, we examined whether ceramide could modulate cellular superoxide anion production using a specific cytochrome c reduction method. Figure 3f confirms that ceramide inhibits basal superoxide production by Jurkat T cells after 16 hours treatment ( $p < 0.05$ ). DPI in itself and in combination with C<sub>2</sub>-ceramide was able to reduce superoxide production further in Jurkat T-cells. Similarly, Figure 3e illustrates that ceramide significantly reduced superoxide production by U937 monocytes, but that this was not further enhanced by coincubation with DPI. As a positive control, the application of exogenous SOD to either U937 monocytes or Jurkat T-cells resulted in total loss of cytochrome c reduction demonstrating absolute dependence on superoxide for the reaction (see Figures 3e & f).

To determine the importance of  $[\text{peroxide}]_{\text{cyt}}$  on outcome, U937 monocytes were pretreated with either of the anti-oxidants NAC or GSH. Cellular GSH rose by 28% and 21% respectively from a basal level of 34.8 nmol per mg of protein after pre-treatment with GSH and NAC respectively, where acivicin pretreatment significantly inhibited the elevation induced by exogenous glutathione ( $p < 0.01$ ). The antioxidants significantly prevented the accumulation of nucleoids in the G<sub>0</sub>/G<sub>1</sub> phase of the cell cycle mediated by 16 hours exposure to 20  $\mu\text{M}$  C<sub>6</sub>-ceramide ( $p < 0.01$ ) and was accompanied by the appearance of sub-

diploid DNA. C<sub>6</sub>-ceramide (20μM) significantly increased the appearance of sub-diploid DNA of U937 monocytes pre-treated with either NAC or GSH compared to no pre-treatment (p<0.05). The percentage nucleoids in the G<sub>0</sub>/G<sub>1</sub> phase of vehicle treated controls were not affected by pre-treatment with NAC (p>0.05) or GSH (p>0.05; see Figure 4b). Further, there was no significant difference in either the inhibitory effects of NAC or GSH on synthetic ceramide mediated G<sub>0</sub>/G<sub>1</sub> nucleoid accumulation (p>0.05; see Figure 4b) or the percentage of actual apoptosis induced by either species in the presence of either anti-oxidant (p>0.05; see Figure 4a). Pre-treatment of U937 monocytes with the anti-oxidants GSH or NAC significantly reduced ΔDCF to approximately -35a.u (p<0.001) after 16 hours vehicle treatment. On addition of 20μM C<sub>6</sub>-ceramide to NAC or GSH pre-treated U937 monocytes, ΔDCF decreased further to approximately -55a.u, and was significantly lower than U937 cells pre-treated with NAC or GSH alone (p<0.01; see Figure 4c). The pre-treatment of Jurkat T-cells with either of the antioxidants NAC or GSH did not increase the kinetics or the magnitude of apoptosis induced by 20μM C<sub>2</sub>-ceramide (see Figure 5a). Treatment of U937 monocytes or Jurkat T-cells with concentrations of either NAC or GSH in excess of 10μM were in themselves cytotoxic (data not shown). Previously we have reported that efflux of oxidised GSH from the cell precedes synthetic ceramide mediated Jurkat T-cell apoptosis and may be a contributory mechanism to apoptosis process [23], however, pre-treatment with the GSH efflux inhibitors L-cystathionine or L-methionine [34] did not affect Jurkat T-cell apoptosis (0-20μM; p>0.05 for each concentration and species; see Figure 5b) or G<sub>0</sub>/G<sub>1</sub> growth arrest in U937 monocytes (Data not shown) induced by C<sub>2</sub>-/C<sub>6</sub>-ceramide, despite protecting cellular glutathione status (U937 cells= 29.83±1.27nmol GSH/mg protein; U937 + 20μM ceramide for 1hour = 25.95±1.61nmolGSH/mg protein; U937 + methionine + 20μM ceramide for 1 hour = 28.7±1.7 nmolGSH/mg protein, n=9).

To determine whether the effects observed in immortalised cells were reproduced in a mixed population of primary cells, T-lymphocytes and monocytes (identified by expression of the antigens CD3 and CD14 respectively) from peripheral whole blood were individually gated and the DCF fluorescence of CD3<sup>+</sup> and CD14<sup>+</sup> populations analysed on a single parameter histogram of FL1 versus count (see Figures 6a & b). The DCF fluorescence of CD3<sup>+</sup> T-cells and CD14<sup>+</sup> monocytes displayed reduced [peroxide]<sub>cyt</sub> following the treatment of whole blood with 20µM C<sub>6</sub>-ceramide when compared to vehicle treated whole blood T-cells or monocytes (see Figures 6c & d).

To further substantiate the observations of reduced [peroxide]<sub>cyt</sub> in response to short chain ceramides obtained in immortalised cell lines and whole blood, primary, resting T-cells were extracted from venous whole blood. Purity (as the percentage of CD3<sup>+</sup> T-cells) was always greater than 94%. Monocytic contamination was quantified simultaneously (CD14 expression) and was always less than 1.5% (data not shown). T-cells were then cultured in RPMI 1640 in the presence or absence of 10µg/ml of PHA to induce activation. T-cell activation was assessed as the percentage of CD3<sup>+</sup>CD25<sup>+</sup> T-cells. Flow cytometry histograms of SS versus FS showed an increase in size of T-cells which was coupled with a significant elevation in CD3<sup>+</sup>CD25<sup>+</sup> levels to 43.62 ± 15.39% positive T-cells (mean ± s.d; n=12) upon activation with PHA for 3 days compared to 2.605 ± 2.082% for resting T-cells (mean ± s.d; n=12; p<0.001).

DNA cell cycle analysis of PHA activated T-cells revealed the appearance of S-phase and G2M phase nucleoids. As expected, resting T-cells possessed no evidence of DNA in the S-phase or G2M phase of the cell cycle (data not shown). A limiting factor in performing the necessary experiments was the number of T-cells obtained from 40mls of blood, typically 10x10<sup>6</sup>, and consequently for experimental purposes half the concentration of cells, 1x10<sup>6</sup>/ml, was used. Following 6 hours treatment with 0-20µM C<sub>2</sub>-ceramide, DNA cell cycle analysis

by flow cytometry revealed no significant accumulation of sub-diploid DNA in either resting ( $p>0.05$ ; see Figure 7a) or activated ( $p>0.05$ ) primary T-cells (see Figure 8a-d). Furthermore, at this time point  $C_2$ -ceramide induced a concentration dependent decrease in DCF fluorescence in both resting and activated T-cells (see Figures 7c & 8e) which was initially significant at a concentration of  $5\mu\text{M}$   $C_2$ -ceramide in both cell types ( $p<0.05$ ). Following 24 hours treatment of resting or activated T-cells with  $5\mu\text{M}$   $C_2$ -ceramide DCF fluorescence was significantly reduced to approximately -10 a.u from vehicle treated controls ( $p<0.05$ ; data not shown) with no significant evidence of sub-diploid DNA ( $p>0.05$ ) at this time point (see Figures 7b & 8g). On extending the incubation to 24 hours,  $C_2$ -ceramide induced a dose dependent increase in the appearance of sub-diploid DNA in resting T-cells, which was first significant at a concentration of  $10\mu\text{M}$  inducing approximately 30% DNA fragmentation ( $p<0.05$ ) and at  $20\mu\text{M}$   $C_2$ -ceramide 32% ( $p<0.01$ ; see Figure 7b). Likewise, in activated T-cells, at 24 hours post-treatment, the extent of DNA fragmentation was identical to that observed in resting T-cells for each concentration of  $C_2$ -ceramide ( $p>0.05$  for each dose; see Figure 8f-i).

Treatment of Jurkat T-cells with CD95L induced a time and dose dependent elevation in apoptosis. Specific apoptosis was initially observed after 4 hours exposure to  $1\mu\text{g/ml}$  ( $p<0.05$ ) and  $5\mu\text{g/ml}$  ( $p<0.05$ ) of CD95L. These concentrations of CD95L mediated maximal elevation in the percentage of specific apoptosis of approximately 70% after 12 ( $p<0.01$ ) and 16 hours ( $p<0.01$ ) respectively, after which a plateau was observed. Incubations of Jurkat T-cells with these concentrations of CD95L did not induce further alterations in the percentage of specific apoptosis following 16 hours treatment ( $p>0.05$ ). There was no significant difference in the maximal percentage specific apoptosis induced by  $1\mu\text{g/ml}$  and  $5\mu\text{g/ml}$  CD95L ( $p>0.05$ ). Treatment of Jurkat T-cells with  $100\text{ng/ml}$  of CD95L failed to induce any significant elevation in the percentage of specific apoptosis ( $p<0.05$ ) for

up to 16 hours. Intermediate concentrations of CD95L (250ng/ml and 500ng/ml) also induced significant time dependent elevations in the specific apoptosis, which were maximal after 16 hours (20%) and 36 hours (55%) respectively and significantly different to the maximal apoptotic response of 70% induced by higher concentrations of CD95L ( $p < 0.001$ ; see Figure 9a).

CD95L induced a transient elevation in endogenous ceramide ( $[\text{ceramide}]_i$ ) levels in a concentration dependent fashion.  $[\text{ceramide}]_i$  increased significantly to approximately 150% ( $p < 0.05$ ) and 180% ( $p < 0.05$ ) of control levels following 30 minutes treatment with 0.5 and 1 $\mu\text{g/ml}$  CD95L. On increasing the incubation period to 1 hour,  $[\text{ceramide}]_i$  was elevated further to approximately 240% ( $p < 0.05$ ) and 320% of control ( $p < 0.01$ ) by 0.5 and 1 $\mu\text{g/ml}$  CD95L respectively. After 4 hours exposure to either 0.5 or 1 $\mu\text{g/ml}$  CD95L  $[\text{ceramide}]_i$  returned to that of control levels ( $p > 0.05$  for both concentrations; see Figure 9b).

Since CD95L mediated an elevation in the intracellular signal transduction molecule ceramide, and considering our observations of reduced  $[\text{peroxide}]_{\text{cyt}}$  in Jurkat T-cells in response to synthetic ceramide, the effects of CD95L on  $[\text{peroxide}]_{\text{cyt}}$  in Jurkat T-cells were consequently examined. CD95L exposure of Jurkat T-cells mediated a decrease in DCF fluorescence.  $\Delta\text{DCF MdX}$  was significantly reduced after 2 hours treatment with 1 $\mu\text{g/ml}$  ( $p < 0.01$ ) and 8 hours following 500ng/ml CD95L ( $p < 0.05$ ; see Figure 9c), which was prior to any significant observations of apoptosis ( $p > 0.05$  for both concentrations; see Figure 9a) and after the accumulation of intracellular ceramide in response to either concentration of CD95L (see Figure 9b). The reduction in  $\Delta\text{DCF MdX}$  occurred with faster kinetics and was of greater magnitude following Jurkat T-cell treatment with 1 $\mu\text{g/ml}$  of CD95L than that observed following treatment with 500ng/ml CD95L. The decrease in  $\Delta\text{DCF MdX}$  following CD95L exposure reached a plateau after 4 and 8 hours treatment with 1 $\mu\text{g/ml}$  and 500ng/ml respectively (see Figure 9c).

## Discussion.

Controversially, it is reported here that the application of short chain ceramides to T-cells or monocytes induces a loss in cytosolic peroxide ( $[\text{peroxide}]_{\text{cyt}}$ ) levels. This is in contrast to the direct effects of synthetic short chain ceramides on the mitochondria that mediate an elevation in mitochondrial peroxide ( $[\text{peroxide}]_{\text{m}}$ ) production, as described previously by us [23] and by others [21, 22]. Collectively, this supports the notion that ceramide may differentially modulate the redox state at discrete sub-cellular compartments [35]. Indeed, several authors have recently suggested that ROS may inhibit caspase 3 activity, where a reduction in ROS is associated with increased apoptosis [36,37]. Based on our evidence from antioxidant treatment of cells prior to ceramide addition which enhanced the apoptotic response, we hypothesise that in the cellular models utilised here, it is the reduction in  $[\text{peroxide}]_{\text{cyt}}$  that is of primary importance in dictating the cellular response to ceramide rather than its mitochondrial effects. However, a mediator role for the loss of cytosolic peroxide cannot be clearly established from this data.

Jurkat T-cells exposed to synthetic, short chain ceramides show a time dependent elevation in the appearance of fragmented DNA, a marker for apoptosis, as described by others [2-3, 6-8, 12], which was maximal at 8 hours post-treatment with C<sub>2</sub>-ceramide (20 $\mu$ M). We have previously reported no significant difference between the short chain C<sub>2</sub>- and C<sub>6</sub>- ceramides in the induction of apoptosis in T cells [23]. At 16 hours post-treatment, cell death induced by 20 $\mu$ M C<sub>2</sub>-ceramide was also associated with the formation of a sub-population of Jurkat T-cells displaying a reduction in cell size coupled with the loss of membrane permeability evaluated by flow cytometric analysis of the cellular uptake of the membrane impermeable dye PI as the cells enter late apoptosis or secondary necrosis. Unlike Jurkat T-cells, exposure of U937 cells to synthetic ceramide induced an accumulation of nucleoids in the G<sub>0</sub>/G<sub>1</sub> phase of the cell cycle, which is indicative of cell cycle arrest [15-17]

but was not as pronounced as described previously [17]. The observation of growth arrest occurred after 16 hours incubation with 20 $\mu$ M C<sub>2</sub>-ceramide, later than the onset of apoptosis in Jurkat T-cells and was persistent for up to 36 hours. Furthermore, cell size and membrane permeability remained unaltered by ceramide treatment, indicating no induction of necrosis. U937 monocytes are reported to undergo apoptosis upon exposure to concentrations of ceramide in excess of 20 $\mu$ M [12, 22].

Contrary to the observation of ceramide mediated transient elevations in [peroxide]<sub>m</sub> [23], using the cytosolic peroxide sensitive dye DCFH-DA revealed an overall loss in [peroxide]<sub>cyt</sub> prior to the appearance of DNA fragmentation or G0/G1 growth arrest in Jurkat T-cells and U937 monocytes respectively. An apoptotic response in Jurkat T-cells to C<sub>2</sub>-ceramide was preceded by an immediate, almost exponential like reduction in [peroxide]<sub>cyt</sub>. In contrast, where growth arrest was observed in U937 monocytes, the decrease in [peroxide]<sub>cyt</sub> was initially delayed, and fell approximately 40 minutes post-treatment. Additionally, the maximal loss of [peroxide]<sub>cyt</sub> in U937 cells was smaller than that observed in Jurkat T-cells where it was associated with apoptosis. The apparent loss of [peroxide]<sub>cyt</sub> was not due to the leakage of DCFH-DA from the cytosolic environment since cells remained viable as indicated by the minimal uptake of the membrane impermeable dye PI throughout the DCF analysis period. Although 20 $\mu$ M C<sub>2</sub>-ceramide induced a population of Jurkat T-cells with high PI uptake and reduced cell size after 16 hours treatment, these cells were excluded from [peroxide]<sub>cyt</sub> determination as they had undergone secondary necrosis. Lower concentrations of synthetic ceramide (10 $\mu$ M), which did not compromise Jurkat T-cell membrane permeability following 16 hours treatment, showed reduced [peroxide]<sub>cyt</sub> which was not to a level that was associated with apoptosis. The magnitude and kinetics of [peroxide]<sub>cyt</sub> loss may therefore be the true dictator of the cellular responses to synthetic ceramides.

In light of the evidence suggesting that cytoplasmic peroxide levels may play only a minor role in the oxidation of DCF [38,39], where the major catalysts are ferryl containing molecules, we believed it important to adopt a further analytical method that allows direct determination of ROS. Cytochrome c reduction by superoxide anion radical is widely used and accepted as a specific measure of oxidant formation, hence this methodology was adopted to substantiate our findings with DCF. Whilst no change in superoxide production in response to ceramide was recorded at 1 hour, both U937 cells and Jurkat T cells showed a lower capacity to reduce cytochrome at 16hrs, where the effect seen was greater in T-cells. The overall effects of NADPH oxidase inhibition with DPI and ceramide suggest that modulation of NADPH oxidase may be a contributor to the loss of [peroxide]<sub>cyt</sub>, observed, however, the data suggests that other unknown mechanisms may also contribute to this process. Furthermore, the correlation between DPI enhanced ceramide induced apoptosis at 16 hours and loss of [peroxide]<sub>cyt</sub> provides further evidence for the hypothesis that loss of loss of [peroxide]<sub>cyt</sub> is the determining factor in cellular outcome. Clearly more detailed examination of ceramide's potential interaction with the NADPH oxidase system is required.

If the excessive production of [peroxide]<sub>m</sub> were the sole mediator of apoptosis or growth arrest, then a beneficial effect might be expected by pre-treatment of Jurkat T-cells or U937 monocytes respectively with antioxidants. However, we observed that the antioxidants NAC or GSH failed to abrogate synthetic ceramide mediated apoptosis at any time point. Furthermore, the inhibition of GSSG efflux (which was confirmed by demonstrating increased intracellular total GSH) with L-cystathionine or L-methionine did not protect Jurkat T-cells from C<sub>2</sub>-ceramide induced apoptosis despite offering protection against methotrexate (unpublished results) or puromycin [34] treatment. This again suggests that the effects of ceramide are not due to an increase in ROS. Surprisingly, in U937 monocytes NAC and GSH inhibited synthetic ceramide induced G<sub>0</sub>/G<sub>1</sub> growth arrest by driving ceramide treated cells

into apoptosis as indicated by the presence of fragmented DNA. In effect, antioxidants transformed the cellular response of U937 monocytes to ceramide exposure from a cytostatic to cytotoxic response. Reducing the intracellular peroxide levels of U937 monocytes by pre-treatment with antioxidants, which were not in themselves toxic, permits  $[\text{peroxide}]_{\text{cyt}}$  to fall upon ceramide treatment to a level which confers apoptosis. Whilst NAC and GSH treatment alone did cause a reduction in basal DCF fluorescence (-30a.u.), this was insufficient to induce apoptosis (where -55a.u. was associated with apoptosis in T cells), although higher concentrations of either antioxidant were toxic (data not shown). Indeed, several authors have recently suggested that ROS may inhibit caspase 3 activity, where a reduction in ROS below a minimum threshold is associated with increased apoptosis [36,37].

Mansat-de Mas *et al.*, [12] observed elevated fluorescence of a DCFH-DA analogue, C2938, within 20 minutes treatment with C<sub>6</sub>-ceramide that returned to baseline after 30 minutes, whereas Lee & Um, [25] described no alteration in DCF fluorescence following U937 exposure to C<sub>2</sub>-ceramide. However, in our experiments the concentration of C<sub>2</sub>/C<sub>6</sub>-ceramide applied to whole cells encompasses the fluctuation range achieved by endogenous natural ceramides in response to external stimuli [reviewed in 40]. Where other authors have reported massive increases in ROS production at the mitochondria [22] the concentration of C<sub>2</sub>/C<sub>6</sub>-ceramide used were in excess of 5 fold the concentration (per 10<sup>6</sup> cells) that we have used to elicit small transient increases in  $[\text{peroxide}]_{\text{m}}$  [23] or the loss in  $[\text{peroxide}]_{\text{cyt}}$  reported here. The enhanced production of  $[\text{peroxide}]_{\text{cyt}}$  described in response to high doses of ceramides/10<sup>6</sup> cells may therefore be a consequence of ROS leakage from the mitochondria into the cytosol with loss of compartmental redox effects.

The biochemical and molecular processes that lead to cellular responses to various agents analysed in immortalised cell lines are often criticised as they are continually cycling and possess higher metabolic rates. It was therefore of importance to study the cellular and

redox effects of synthetic short chain ceramides on normal, primary human cells. The observation of reduced  $[\text{peroxide}]_{\text{cyt}}$  precedes apoptosis in human  $\text{CD3}^+$  T-cells and  $\text{CD14}^+$  monocytes in peripheral whole blood treated with  $\text{C}_2$ -/ $\text{C}_6$ -ceramide and in purified resting T-cells or PHA activated T-cells *in vitro* supports those data obtained from cell lines. The ability of  $\text{C}_2$ -ceramide to induce apoptosis which was preceded by loss in  $[\text{peroxide}]_{\text{cyt}}$ , was independent of activation state and phase of the cell cycle, where identical levels of  $[\text{peroxide}]_{\text{cyt}}$  loss and DNA fragmentation were observed in resting and PHA activated T-cells. Resting T-cells possessed only DNA that was in the G0 phase of the cell cycle whereas PHA activated T-cells displayed the appearance of a small number of S-phase and G2M phase nucleoids, indicating progression through the cell cycle. In contrast, under identical culture conditions and treatments, Mengabas *et al.*, [41] reported that  $\text{C}_2$ -ceramide killed normal human T-lymphocytes via a non-apoptotic mechanism that was prevented by PHA activation. In the data described herein, the membrane permeability of resting and activated primary human T-cells treated with  $\text{C}_2$ -ceramide (0-20 $\mu\text{M}$ ) was not compromised at 6 hours post-treatment when analysed for uptake of the membrane impermeable dye PI by flow cytometry indicating that necrosis did not contribute to the death process (Data not shown).

In an attempt to analyse the effects of intrinsic endogenous ceramide generation on  $[\text{peroxide}]_{\text{cyt}}$ , Jurkat T-cells were treated with the known inducer of ceramide accumulation, CD95L [6-8]. Herein, we have shown that Jurkat T-cell treatment with CD95L leads to an accumulation of ceramide within 30 minutes, which rose further at 1 hour. This was followed by a reduction in  $[\text{peroxide}]_{\text{cyt}}$  prior to the appearance of apoptosis. Whilst the extent of apoptosis that we observed following treatment with 1 $\mu\text{g}/\text{ml}$  or 0.5 $\mu\text{g}/\text{ml}$  CD95L was similar to that mediated by 20 $\mu\text{M}$   $\text{C}_2$ -ceramide, the kinetics of the appearance of fragmented DNA were slower and correspondingly the magnitude reduction in  $[\text{peroxide}]_{\text{cyt}}$  generation was less and occurred more slowly. In contrast, others have shown that whilst

CD95 receptor stimulation induced ceramide formation in human glioma cells via the activation of A-SMase, no ROS formation was observed and the ensuing apoptosis unaffected by antioxidants [20]. Similarly, L929 cells expressing the CD95 receptor undergo CD95 induced apoptosis which is not inhibitable by antioxidants [42]. These observations are in contrast to the elevation in DCF fluorescence reported in IL-1 $\beta$ /TNF $\alpha$  activated peripheral blood monocytes [PBM] prior to apoptosis induced by CD95L exposure, both of which were inhibitable by antioxidants [43], and other studies which suggested that CD95 induces ROS generation via stimulation of the NADPH oxidase system [44,45]. Others have also shown neuroglioma cells overexpressing Cu or ZnMnSOD showed marked attenuation of CD95 induced apoptosis, that catalase treatment inhibited CD95 induced apoptosis of normal neurogliomas [46], and that NAC or GSH inhibited CD95L induced apoptosis in HL60 variant HL-525, in the absence of an elevation in endogenous ceramides [47]. These discrepancies may exist due to differences in cell lineage or the degree of saturation and length of fatty acid chain between endogenous ceramides generated by ligands such as FAS and synthetic exogenously applied short chain ceramides. However, during preparation of this manuscript, Aronis et al. have also published the observation of a decrease in ROS production in response to CD95 receptor stimulation in Jurkat T-cells that correlates with enhanced cell death [48], further supporting the impact of the observations reported here.

We have observed that short chain ceramide manipulates the intracellular redox state through mitochondrial and non-mitochondrial pathways. [peroxide]<sub>m</sub> generation may be important in parallel, but acting within a different sub-cellular compartment, to ceramide induced loss of [peroxide]<sub>cyt</sub>. The loss of [peroxide]<sub>cyt</sub> in response to short chain ceramides in the immortalised cell lines of U937 monocytes and Jurkat T-cells has been reproduced in primary human cells of identical lineage, indicating that the effects are not related to cellular immortality. Furthermore, the data presented here, taken together with our previous

observations [23] indicate the existence of discrete redox sensitive entities which may be targeted and manipulated by ceramide to produce independent responses.

## Acknowledgements

The authors gratefully acknowledge Aston University for endowment of a studentship for DCP, and thank Dr Mark Burkitt, Gray Laboratories, for helpful discussion.

## References.

1. Gamard, C., Dbaibo, G., Liu, B., Obeid, L. and Hannun, Y. (1997). Selective involvement of ceramide in cytokine-induced apoptosis. *J. Biol. Chem.* **272**, 16474-16481.
2. Liu, B., Andreieu-Abadie, N., Levade, T., Zhang, P., Obeid, L. and Hannun, Y. (1998). Glutathione regulation of neutral sphingomyelinase in Tumour necrosis factor- $\alpha$  induced cell death. *J. Biol. Chem.* **273**, 11313-11320.
3. Obeid, L., Linardic, C., Karolak, L. and Hannun, Y. (1993). Programmed cell death induced by ceramide. *Science* **259**, 1769-1771.
4. Verheij, M., Bose, R., Lin, X., Yao, B., Jarvis, W., Grant, S., Birrer, M., Szabo, E., Zon, L., Kyriakis, J., Haimovitz-Friedman, A., Fuks, Z. and Kolesnick, R. (1996). Requirement for ceramide initiated SAPK/JNK signaling in stress-induced apoptosis. *Nature* **380**, 75-79.
5. Andrieu, N., Salvayre, R. and Levade, T. (1994). Evidence against involvement of the acid lysosomal sphingomyelinase in the tumor-necrosis-factor- and interleukin-1-induced sphingomyelin cycle and cell proliferation in human fibroblasts. *Biochem J.* **303**, 341-345.
6. Cifone, M., De Maria, R., Roncaioli, P., Rippo, M., Azuma, M., Lanier, L., Santoni, A. and Testi, R. (1993). Apoptotic signalling through CD95 (Fas/Apo-1) activates an acidic sphingomyelinase. *J. Exp. Med.* **177**, 1547-1552.
7. Gulbins, E., Bissonnette, R., Mahboubi, A., Martin, S., Nishioka, W., Brunner, T., Baier, G., Baier-Bitterlich, G., Byrd, C., Lang, F., Kolesnick, R., Altman, A. and Green, D. (1995). FAS-induced apoptosis is mediated via a ceramide-initiated RAS signalling pathway. *Immunity* **2**, 341-351.
8. Tepper, A., Boesen-De Cock, J.G.R., De Vries, E., Borst, J. And Van Blitterswijk, W.J. (1997). CD95/Fas-induced ceramide formation proceeds with slow kinetics and is not blocked by caspase-3/CPP32 inhibition. *J. Biol. Chem.* **272**, 24308-24312.

9. Santana, P., Peña, L., Haimovitz-Friedman, A., Martin, S., Green, D., Mcloughlin, M., Cordon-Cardo, C., Schuchman, E., Fuks, Z. and Kolesnick, R. (1996). Acid sphingomyelinase-deficient human lymphoblasts and mice are defective in radiation-induced apoptosis. *Cell* **86**, 189-199.
10. Boland, M., Foster, S. and O'Neill, L. (1997). Daunorubicin activates NF $\kappa$ B and induces  $\kappa$ B-dependent gene expression in HL-60 promyelocytic and Jurkat T lymphoma cells. *J. Biol. Chem.* **272**, 12952-12960.
11. Bose, R., Verheij, M., Haimovitz-Friedman, A., Scotto, K., Fuks, Z. and Kolesnick, R. (1995). Ceramide synthase mediates daunorubicin-induced apoptosis: an alternative mechanism for generating death signals. *Cell* **82**, 405-414.
12. Mansat-De Mas, V., Bezombes, C., Quillet-Mary, A., Bettaieb, A., De Thonel D'orgeix, A., Laurent, G. and Jaffr  zou, J.-P. (1999). Implication of radical oxygen species in ceramide generation, c-Jun terminal kinase activation and apoptosis induced by daunorubicin. *Mol. Pharm.* **56**, 867-874.
13. Mackichan, M. and Defranco, A. (1999). Role of ceramide in lipopolysaccharide (LPS)-induced signalling. *J. Biol. Chem.* **274**, 1767-1775.
14. Hanna, A., Chan, E., Xu, J., Stone, J. and Brindley, D. (1999). A novel pathway for Tumour necrosis factor- $\alpha$  and ceramide signaling involving sequential activation of tyrosine kinase p21ras, and phosphatidylinositol 3-kinase. *J. Biol. Chem.* **274**, 12722-12729.
15. Dbaibo ,G.S., Pushkareva, M.Y., Jayadev, S., Schwarz, J.K., Horowitz, J.M., Obeid, L.M., Hannun, Y.A.(1995). Retinoblastoma gene product as a downstream target for a ceramide-dependent pathway of growth arrest. *Proc Natl Acad Sci U S A.* **92**, 1347-1351.
16. Jayadev, S., Liu, B., Bielawska, A., Lee, J., Nazaire, F., Pushkareva, M., Obeid, L. and Hannun, Y. (1995). Role of ceramide in cell cycle arrest. *J. Biol. Chem.* **270**, 2047-2052.
17. Ragg, S., Kaga, S., Berg, K. & Ochi, A. (1998). The mitogen-activated protein kinases pathway inhibits ceramide-induced terminal differentiation of a human monoblastic leukemia cell line, U937. *J. Immunol.* **161**, 1390-1398.
18. Venable, M., Lee, J., Smyth, M., Bielawska, A. and Obeid, L. (1995). Role of ceramide in cellular senescence. *J. Biol. Chem.* **270**, 30701-30708.
19. Liu, B. and Hannun, Y. (1997). Inhibition of neutral magnesium-dependent sphingomyelinase by glutathione. *J. Biol. Chem.* **272**, 16281-16287.
20. Sawada, M., Nakashima, S., Kiyono, T., Yamada, J., Hara, S., Nakagawa, M., Shinoda, J. and Sakai, N. (2002). Acid sphingomyelinase activation requires caspase-8 but not p53 nor

reactive oxygen species during Fas-induced apoptosis in human glioma cells. *Exp. Cell Res.* **273**, 157-168.

21. García-Ruiz, C., Colell, A., Mari, M., Morales, A. and Fernández-Checa, J. (1997). Direct effect of ceramide in the mitochondrial electron transport chain leads to generation of reactive oxygen species. *J. Biol. Chem.* **272**, 11369-11377.

22. Quillet-Mary, A., Jaffrézou, J.-P. , Mansat, V., Bordier, C., Naval, J. and Laurent, G. (1997). Implication of mitochondrial hydrogen peroxide generation in ceramide-induced apoptosis. *J. Biol. Chem.* **272**, 21388-21395.

23. Phillips, D.C., Allen, K. and Griffiths, H.R. (2002). Synthetic ceramides induce growth arrest or apoptosis by altering cellular redox status with differing kinetics. *Arch. Biochem. Biophys.* **407**, 15-24.

24. Schulze-Osthoff, K., Bakker, A., Vanhaesebroeck, B., Beyaert, R., Jacob, W. and Friers, W. (1992). Cytotoxic activity of tumour necrosis factor is mediated by early damage of mitochondrial functions. *J. Biol. Chem.* **267**, 5317-5323.

25. Lee, B. and Um, H.-D. (1999). Hydrogen peroxide suppresses U937 cell death by two different mechanisms depending on its concentration. *Exp. Cell Res.* **248**, 430-438.

26. Fang, W., Rivard, J.J., Ganser, J., Lebien, T.W., Nath, K.A., Mueller, D.L. and Behrens, T.W. (1995). Bcl-x<sub>L</sub> rescues WEHI 231 B lymphocytes from oxidant-mediated death following diverse apoptotic stimuli. *J. Immunol.* **155**, 66-75.

27. Nicolletti, I., Migliorati, G., Pagliaccii, M., Grignani, F. and Riccardi, C. (1991). A rapid and simple method for measuring thymocyte apoptosis by propidium iodide staining and flow cytometry. *J. Immunol. Methods* **139**, 271-279.

28. Bass, D., Parce, J., Dechatelet, L., Szejda, P., Seeds, M. and Thomas, M. (1983). Flow cytometric studies of oxidative product formation by neutrophils: a graded response to membrane stimulation. *J. Immunol.* **130**, 910-917.

29. Tietze, F. (1969). Enzymic method for quantitative determination of nanogram amounts of total and oxidized glutathione: applications to mammalian blood and other tissues. *Anal. Biochem.* **27**, 502-522.

30. Smith, P., Krohn, R., Hermanson, G., Mallia, A., Gartner, F., Provenzano, M., Fujimoto, E., Goeke, N., Olson, B. and Klenk, D. Measurement of protein using bicinchoninic acid. (1985). *Anal. Biochem.* **150**, 76-85.

31. Bligh, E. and Dyer, W. (1959). A rapid method of total lipid extraction. *Can. Biochem. J. Physiol.* **37**, 911-917.

32. Preiss, J., Loomis, C., Bishop, W., Stein, R., Niedel, J. and Bell, R. (1986). Quantitative

measurement of sn-1,2-diacylglycerols present in platelets, hepatocytes, and ras- and sis-transformed normal rat kidney cells. *J. Biol. Chem.* **261**, 8597-8600.

33. Bielawska, A., Perry, D. and Hannun, Y. (2001). Determination of ceramides and diglycerides by the diglyceride kinase assay. *Anal. Biochem.* **298**, 141-150.

34. Ghibelli, L., Fanelli, C., Rotilio, G., Lafavia, E., Coppola, S., Colussi, C., Civitareale, P. and Ciriolo, M. (1998). Rescue of cells from apoptosis by inhibition of active GSH extrusion. *FASEB J.* **12**, 479-486.

35. Pani, G., Bedogni, B., Colavitti, R., Anzevino, R., Borrello, S., Galeotti, T. (2001). Cell compartmentalization in redox signaling. *IUBMB Life* **52**, 7-16

36. Hampton, M.B., Stamenkovic, I. And Winterbourn, C.C. (2002) Interaction with substrate sensitises caspase-3 to inactivation by hydrogen peroxide. *FEBS letts.* **517**, 229-232.

37. Lee, W-R., Shen, S-G., Lin, H-Y., Hou, W-C., Yong, L-L., Chen, Y-C. (2002) Wogonin and fisetin induce apoptosis in human promyeloleukemic cells, accompanied by a decrease of reactive oxygen species, and activation of caspase 3 and Ca(2+)-dependent endonuclease. *Biochem. Pharmacol.* **63**, 225-236.

38. Rota C., Chignell C.F, Mason R.P. (1999). Evidence for free radical formation during the oxidation of 2'-7'-dichlorofluorescin to the fluorescent dye 2'-7'-dichlorofluorescein by horseradish peroxidase: possible implications for oxidative stress measurements. *Free Radic Biol Med.* **27**, 873-881.

39. Burkitt M.J., Wardman P. (2001). Cytochrome C is a potent catalyst of dichlorofluorescin oxidation: implications for the role of reactive oxygen species in apoptosis. *Biochem Biophys Res Commun.* **282**, 329-333.

40. Hannun, Y.A. and Luberto, C. (2000) Ceramide in the eukaryotic stress response. *Trends Cell Biol.* **10**, 73-80.

41. Mengubas, K., Fahey, A., Lewin, J., Mehta, A., Hoffbrand, A. and Wickremasinghe, R. (1999). Killing of T lymphocytes by synthetic ceramide is by a nonapoptotic mechanism and is abrogated following mitogenic activation. *Exp. Cell Res.* **249**, 116-122.

42. Schulze-Osthoff, K., Krammer, P.H., Droge, W. (1994). Divergent signalling via APO-1/Fas and the TNF receptor, two homologous molecules involved in physiological cell death. *EMBO J.* **13**, 4587-4596.

43. Um, H.-D., Orenstein, J. and Wahl, S. (1996). Fas mediated apoptosis in human monocytes by a reactive oxygen intermediate dependent pathway. *J. Immunol.* **156**, 3469-3477.

44. Suzuki, Y., Ono, Y. and Hirabayashi, Y. (1998). Rapid and specific reactive oxygen

species generation via NADPH oxidase activation during Fas-mediated apoptosis. *FEBS Lett.* **425**, 209-212.

45. Suzuki, Y. and Ono, Y. (1999). Involvement of reactive oxygen species produced via NADPH oxidase in tyrosine phosphorylation in human B- and T-lineage lymphoid cells. *Biochem. Biophys. Res. Commun.* **255**, 262-267.

46. Jayanthi, S., Ordonez, S., McCoy, M. and Cadet, J. (1999). Dual mechanism of Fas-induced cell death in neuroglioma cells: a role for reactive oxygen species. *Brain Res. Mol. Brain Res.* **72**, 158-165.

47. Laouar, A., Glesne, D. and Huberman, E. (1999). Involvement of protein kinase C- $\beta$  and ceramide in tumour necrosis factor- $\alpha$ -induced but not Fas-induced apoptosis of human myeloid leukemia cells. *J Biol Chem.* **274**, 23526-23534.

48. Aronis, A., Melendez, J.A., Golan, O., Shilo, S., Dicter, N., Tirosh, O. (2003). Potentiation of Fas-mediated apoptosis by attenuated production of mitochondria-derived reactive oxygen species. *Cell Death Differ.* **10**, 335-344.

## Tables and Figures

### **Figure 1. Loss of endogenous, cytosolic peroxide from Jurkat T-cells precedes apoptosis.**

Jurkat T-cells ( $2 \times 10^6$ /ml) were serum starved for 4 hours prior to the addition of  $C_2$ -ceramide for 0-36 hours. Incubations were performed at  $37^\circ\text{C}$  in a 95% air, 5%  $\text{CO}_2$  humidified atmosphere. For DNA cell cycle analysis by flow cytometry (a), treatments were terminated by washing the cells twice with ice cold PBS, cell pellets resuspended in 1ml of hypotonic fluorochrome solution and incubated in the dark at  $4^\circ\text{C}$  overnight. The sub-diploid DNA content of 20,000 nucleoids from each sample was analysed on a gated histogram of FL3 (propidium iodide; PI) versus count. The data are presented as the mean  $\pm$  s.e.m of at least 7 individual experiments, expressed as the percentage specific apoptosis according to the formula specific apoptosis =  $(T-C)/(100-C) \times 100$ , where T equals the percentage of apoptotic events from treated cells, and C equals the percentage of apoptotic events from control cells. For analysis of cytosolic peroxide levels (b), 40 minutes before termination of the incubation period, cell samples were loaded with  $50\mu\text{M}$  DCFH-DA. At the end of the treatment period, samples were analysed immediately for DCF fluorescence by flow cytometry as described in materials and methods and the median X (MdX) of 10,000 cells recorded. Data is expressed as the mean  $\pm$  s.e.m of at least 3 individual experiments.

### **Figure 2. $C_6$ -ceramide induced growth arrest in U937 monocytes is preceded by a loss in cytosolic peroxide.**

U937 cells ( $2 \times 10^6$ /ml) were serum starved in RPMI 1640 for 4 hours prior to the addition  $0$ - $20\mu\text{M}$   $C_6$ -ceramide and incubated in a humidified 5%  $\text{CO}_2$ , 95% air atmosphere at  $37^\circ\text{C}$  for 8 - 36 hours. For DNA cell cycle analysis by flow cytometry (a), treatments were terminated by washing the cells twice with ice cold PBS, cell pellets resuspended in 1ml of hypotonic fluorochrome solution and incubated in the dark at  $4^\circ\text{C}$  overnight. The sub-diploid DNA content (% actual apoptosis) of 20,000 nucleoids from each sample was analysed on a gated histogram of FL3 (propidium iodide; PI) versus count. The percentage G0/G1 content of DNA cell cycles were quantified using MultiCycle<sup>TM</sup> for Windows (Phoenix Flow Systems, San Diego, U.S.A.). The data are presented as the arithmetic mean percents  $\pm$  s.e.m of at least 3 individual experiments. \* indicate  $p < 0.05$  or \*\* indicate  $p < 0.01$  compared to vehicle treatment by one way ANOVA followed by Dunnett's multiple comparison test. For analysis of cytosolic peroxide levels (b), U937 monocytes were treated as described in Figure 1. Data is expressed as the mean  $\pm$  s.e.m of at least 3 individual experiments.

**Figure 3. Ceramide-induced reduction of cytosolic peroxide is not directly related to NADPH oxidase inhibition of superoxide generation.** U937 or Jurkat T cells ( $2 \times 10^6$ /ml) were serum starved in RPMI 1640 for 4 hours with or without 10  $\mu$ M diphenylene iodonium (DPI) prior to the addition 20  $\mu$ M C<sub>2</sub>-ceramide for 16 hours at 37°C. Prior to termination of the incubation period, cell samples were loaded with 50  $\mu$ M DCFH-DA for 40 minutes as described in Figure 1. Samples were analysed immediately for DCF fluorescence by flow cytometry and the median X (MdX) of 10,000 cells recorded (a & b). The same samples were also analysed for evidence of apoptosis (c & d) by DNA cell cycle analysis as described in Figure 2. U937 or Jurkat T cells ( $10^7$ /ml) were resuspended in phenol red free HBSS containing glucose with or without 10  $\mu$ M diphenylene iodonium (DPI) or 30 U/ml superoxide dismutase (SOD) in the presence of cytochrome c (160  $\mu$ M) prior to the addition 20  $\mu$ M C<sub>2</sub>-ceramide for 16 hours at 37°C. Cytochrome c reduction was monitored at 550nm and the superoxide released calculated as described in the materials and methods (e & f). All data are presented as the mean  $\pm$  s.e.m of 3 individual experiments and where \* ( $p < 0.05$ ), \*\* ( $p < 0.01$ ) or \*\*\* ( $p < 0.001$ ) represents significant differences from vehicle treated control samples and + ( $p < 0.05$ ) or +++ ( $p < 0.001$ ) indicates significant difference from C<sub>2</sub>-ceramide treated cells.

**Figure 4. Anti-oxidants drive synthetic ceramide treated U937 monocytes into apoptosis rather than growth arrest.** U937 cells ( $2 \times 10^6$ /ml) were serum starved in RPMI 1640 for 4 hours with or without 10mM N-acetylcysteine (NAC) or 10mM glutathione (GSH) prior to the addition 20  $\mu$ M C<sub>2</sub>-/C<sub>6</sub>-ceramide for 16 hours at 37°C. Samples were prepared for DNA cell cycle analysis as described in Figure 2. The sub-diploid DNA content recorded to represent the percentage actual apoptosis (a). The percentage G0/G1 content of DNA (b) was quantified using MultiCycle™ for Windows (Phoenix Flow Systems, San Diego, U.S.A.). Data are presented as mean percentage  $\pm$  s.e.m of 3 individual experiments. \* ( $p < 0.05$ ), \*\* ( $p < 0.01$ ) or \*\*\* ( $p < 0.001$ ) indicate significant difference of samples pre-treated with NAC or GSH compared to no pre-treatment by one way ANOVA followed by Tukey's multiple comparison test. For analysis of cytosolic peroxide (c), 50  $\mu$ M DCFH-DA was added to each sample 40 minutes prior to the end of the incubation period. At 16 hours, cell samples were analysed immediately for DCF fluorescence by flow cytometry as described in Figure 1. Data are presented as mean percentages  $\pm$  s.e.m ( $n=3$ ). \*\* ( $p < 0.01$ ) indicate significant difference between samples treated with 20  $\mu$ M C<sub>6</sub>-ceramide with GSH or NAC pre-treatment compared to no pre-treatment, xxx ( $p < 0.001$ ) represents significant difference of test samples from

control treated cells with no pre-treatment and ++ ( $p < 0.01$ ) indicates significant difference between test and control samples both pre-treated with NAC or GSH compared to one way ANOVA followed by Dunnett's multiple comparison test.

**Figure 5. Antioxidants do not protect Jurkat T-cells from ceramide mediated apoptosis.**

Jurkat T-cells ( $2 \times 10^6$ /ml) were serum starved in RPMI 1640 for 4 hours with or without 10mM N-acetylcysteine (NAC) or 10mM glutathione (GSH) prior to the addition 20 $\mu$ M C<sub>2</sub>-ceramide for 1 to 12 hours (a). Alternatively, cell suspensions were treated with 10mM L-cystathionine or L-methionine prior to treatment with 0-20 $\mu$ M C<sub>2</sub>-/C<sub>6</sub>-ceramide for 16 hours (b). All incubations were performed in a humidified 5% CO<sub>2</sub>, 95% air atmosphere at 37°C for 36 hours. Experiments were terminated by washing with ice cold PBS. Cell pellets were resuspended in 1ml of hypotonic fluorochrome solution as described in materials and methods prior to DNA cell cycle analysis by flow cytometry. 20,000 nucleoids were counted per sample. Data are presented as mean percentages  $\pm$  s.e.m of between 3 and 7 individual experiments. Data was analysed for significant difference between samples pre-treated with NAC, GSH, L-cystathionine or L-methionine compared to no pre-treatment by one-way ANOVA followed by Tukey's multiple comparison test.

**Figure 6. Treatment of whole blood with C<sub>6</sub>-ceramide reduces the cytosolic peroxide concentration of CD3<sup>+</sup>ve T-lymphocytes and CD14<sup>+</sup> monocytes.**

Venous blood was obtained from healthy consenting adult humans and treated with 20 $\mu$ M C<sub>6</sub>-ceramide for 2 hours at 37°C with rotation. Reactions were terminated by incubation on ice with simultaneous treatment with the fluorescently tagged monoclonal antibodies CD3-PE and CD14-CY5PE, and 50 $\mu$ M DCFH-DA for 30 minutes. Red blood cells were lysed and leukocytes fixed as described in methods. Samples were analysed by flow cytometry and the DCF fluorescence of the CD3<sup>+</sup> population and CD14<sup>+</sup> population quantified. Shown are typical flow cytometric histograms of (a) CD3-PE (FL2) versus SS, the highly fluorescent CD3<sup>+</sup> cell population isolated and gated 'Y', (b) CD14-CY5PE (FL4) versus SS, the highly fluorescent CD14<sup>+</sup> cell population isolated and gated 'Z', (c) DCF (FL1) versus count of the gated CD3<sup>+</sup> population 'Y' and (e) DCF (FL1) versus count of the gated CD14<sup>+</sup> population 'Z'. Grey fill represent the DCF fluorescence of CD3<sup>+</sup> (c) or CD14<sup>+</sup> (d) populations respectively from vehicle treated whole blood, black outlines with no fill represent the DCF fluorescence obtained from whole blood treated with 20 $\mu$ M C<sub>6</sub>-ceramide. Results are

representational of 3 independent experiments. Histogram overlay was performed using WinMDI 2.8.

**Figure 7. Synthetic short chain ceramides induce cytosolic peroxide loss in resting human T-lymphocytes prior to the appearance of DNA fragmentation.** Primary human peripheral blood T-lymphocytes were extracted by density centrifugation and purified by negative isolation. T-cells were cultured for 3 days in RPMI 1640 (10% FCS, 1% P/S) at a concentration of  $2 \times 10^6$ /ml. T-cells ( $1 \times 10^6$ /ml) were then serum starved in RPMI 1640 for 4 hours prior to exposure to  $C_2$ -ceramide (0-20 $\mu$ M) for 6 hours (a & c) or 24 hours (b). For the quantification of apoptosis (a & b), samples were resuspended in hypotonic fluorochrome solution and incubated overnight in the dark at 4°C prior to DNA cell cycle analysis by flow cytometry as described in material and methods. The percentage actual apoptosis was calculated from the sub-diploid content of 20,000 nucleoids per sample. For analysis of cytosolic peroxide levels (c), 40 minutes before termination of incubation period, cell samples were loaded with 50 $\mu$ M of DCFH-DA. At the end of the treatment period, samples were analysed immediately for DCF fluorescence by flow cytometry as described in materials and methods, and the median X (MdX) of 10,000 cells were recorded.  $\Delta$ DCF represents the change in DCF MdX of test samples from vehicle controls. The data are presented as the arithmetic mean  $\pm$  s.d of at least 3 individual experiments. All cell culture and treatments were performed at 37°C in a humidified 95% air, 5% CO<sub>2</sub> atmosphere. Statistical analysis was performed by one way ANOVA followed by Dunnett's post *hoc* test analysis, where \*\* (p<0.01) represents significant difference from controls. Arbitrary units, a.u. NS represents no significant difference between vehicle treated controls and tests.

**Figure 8. Synthetic short chain ceramides induce cytosolic peroxide loss in activated human T-lymphocytes prior to the appearance of DNA fragmentation.** Primary human peripheral blood T-lymphocytes were extracted by density centrifugation and purified by negative isolation (Dyna). T-lymphocytes were cultured for 3 days in RPMI 1640 (10% FCS, 1% P/S) containing 10 $\mu$ g PHA per  $2 \times 10^6$ /ml T-cells. T-cells were then serum starved in RPMI 1640 for 4 hours prior to exposure to  $C_2$ -ceramide (0-20 $\mu$ M) for 6 (a-e) or 24 hours (f-i). For DNA cell cycle analysis by flow cytometry, samples were washed twice with ice cold PBS, resuspended in hypotonic fluorochrome solution and incubated overnight in the dark at 4°C. The sub-diploid region of 20,000 nucleoids from each sample were evaluated on

gated histograms count versus FL3 (propidium iodide; PI). Shown are DNA cell cycle histograms obtained from samples treated with vehicle (a & f), 5 $\mu$ M (b & g), 10 $\mu$ M (c & h) or 20 $\mu$ M (d & i) C<sub>2</sub>-ceramide. Numbers represent the mean percentage of sub-diploid DNA  $\pm$  s.d of at least 3 individual experiments. Data was analysed for statistical difference by one way ANOVA followed by Dunnett's multiple comparison test where \* (p<0.05) and \*\* (p<0.01) represents significant difference from controls. For analysis of cytosolic peroxide levels (e), 40 minutes before termination of incubation period, cell samples were loaded with 50 $\mu$ M of DCFH-DA. At the end of the treatment period, samples were analysed immediately for DCF fluorescence by flow cytometry as described in materials and methods and the median X (MdX) of 10,000 cells were recorded. Shown is an overlay of DCF histograms from T-cells treated with vehicle, 5 $\mu$ M, 10 $\mu$ M or 20 $\mu$ M C<sub>2</sub>-ceramide. Histogram overlay was performed using WinMDI 2.8. Results are representative of those obtained from at least 3 individual experiments. All cell culture and treatments were performed at 37°C in a humidified 5% CO<sub>2</sub>, 95% air atmosphere.

**Figure 9. CD95 induced apoptosis in Jurkat T-cells is preceded by endogenous ceramide production and loss in cytosolic peroxide.** Jurkat T-cells (2x10<sup>6</sup>/ml) were serum starved for 4 hours prior to the addition of CD95 ligand (CD95L; 0-5 $\mu$ g/ml) for 0-24 hours. Incubations were performed at 37°C in a 95% air, 5% CO<sub>2</sub> humidified atmosphere and terminated by washing the cells twice with ice cold PBS prior to further experimental manipulation. (a) For quantification of apoptosis, samples were prepared and analysed as described in Figure 1. (b) Lipids were extracted and endogenous ceramide quantified against a standard curve of known ceramide concentrations by the DAGK assay as described. (c) For analysis of cytosolic peroxide levels, 40 minutes before termination of incubation period, cell samples were loaded with 50 $\mu$ M DCFH-DA. At the end of the treatment period, samples were analysed immediately for DCF fluorescence by flow cytometry as described in materials and methods and the median X (MdX) of 10,000 cells were recorded.  $\Delta$ DCF MdX represents the difference in MdX DCF of CD95 treated cells from that of vehicle treated cells for each time point. The data are presented as the mean  $\pm$  s.e.m. of between 3 and 5 individual experiments, a.u. = arbitrary units.

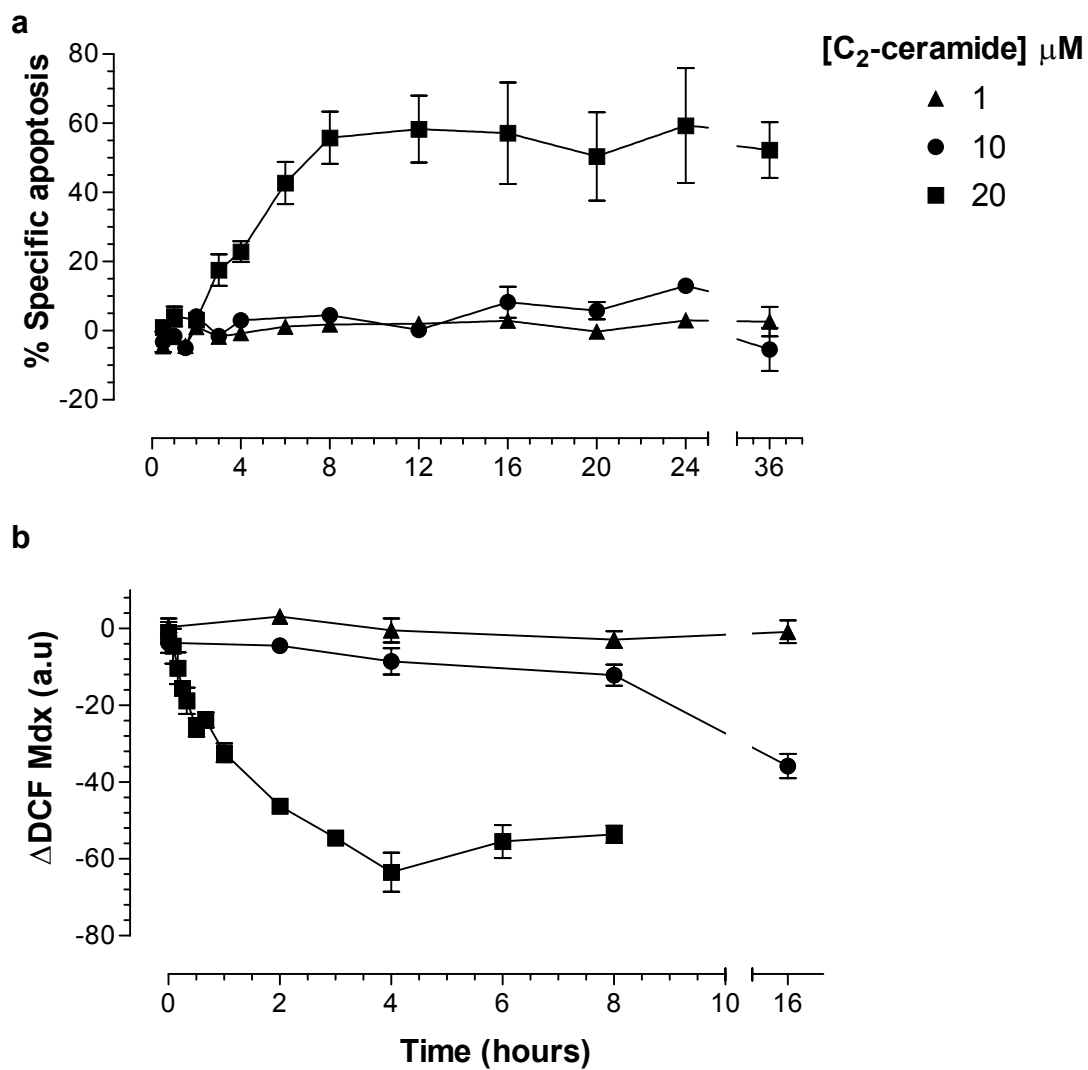


Figure 1.

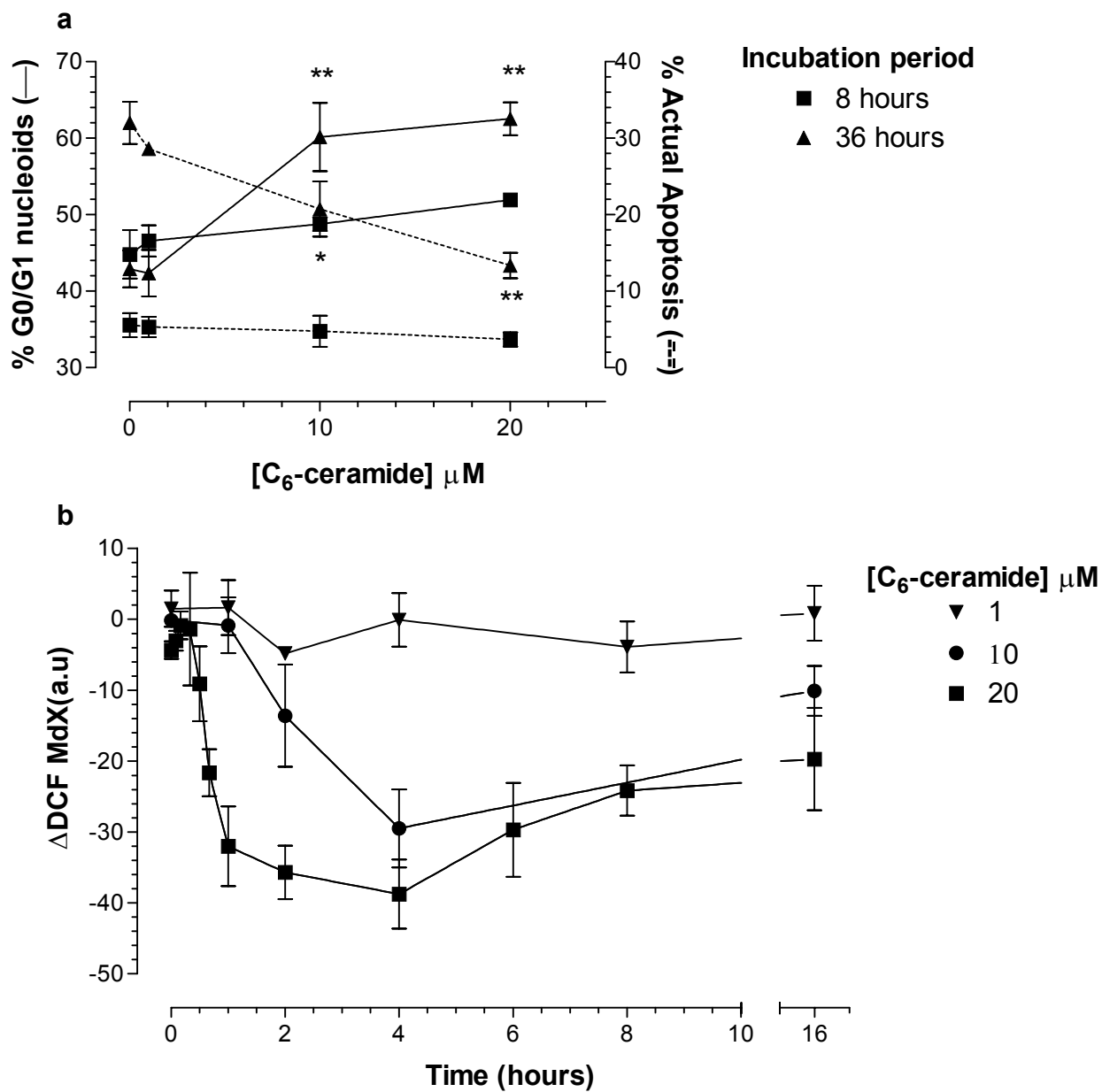


Figure 2.

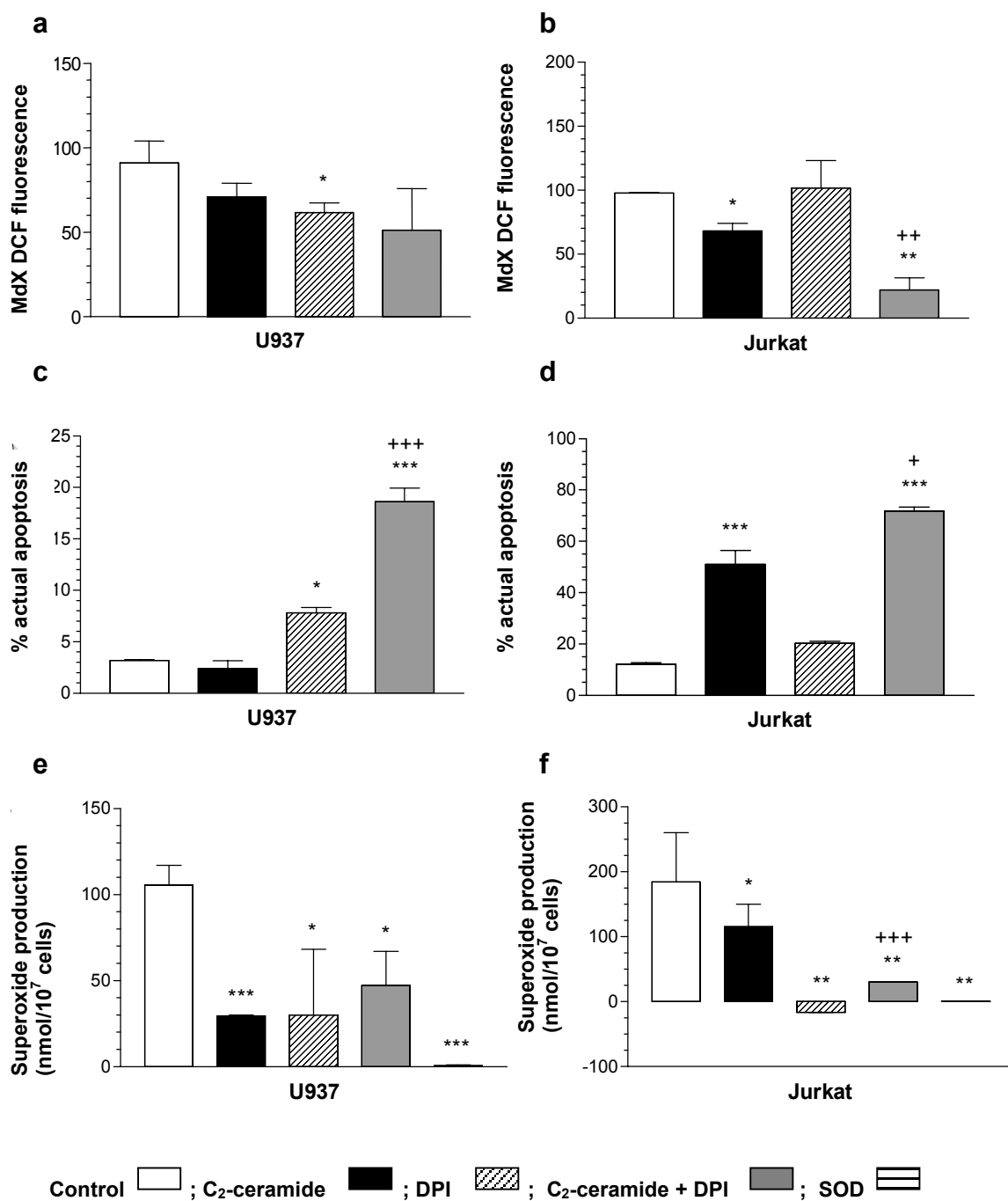


Figure 3.

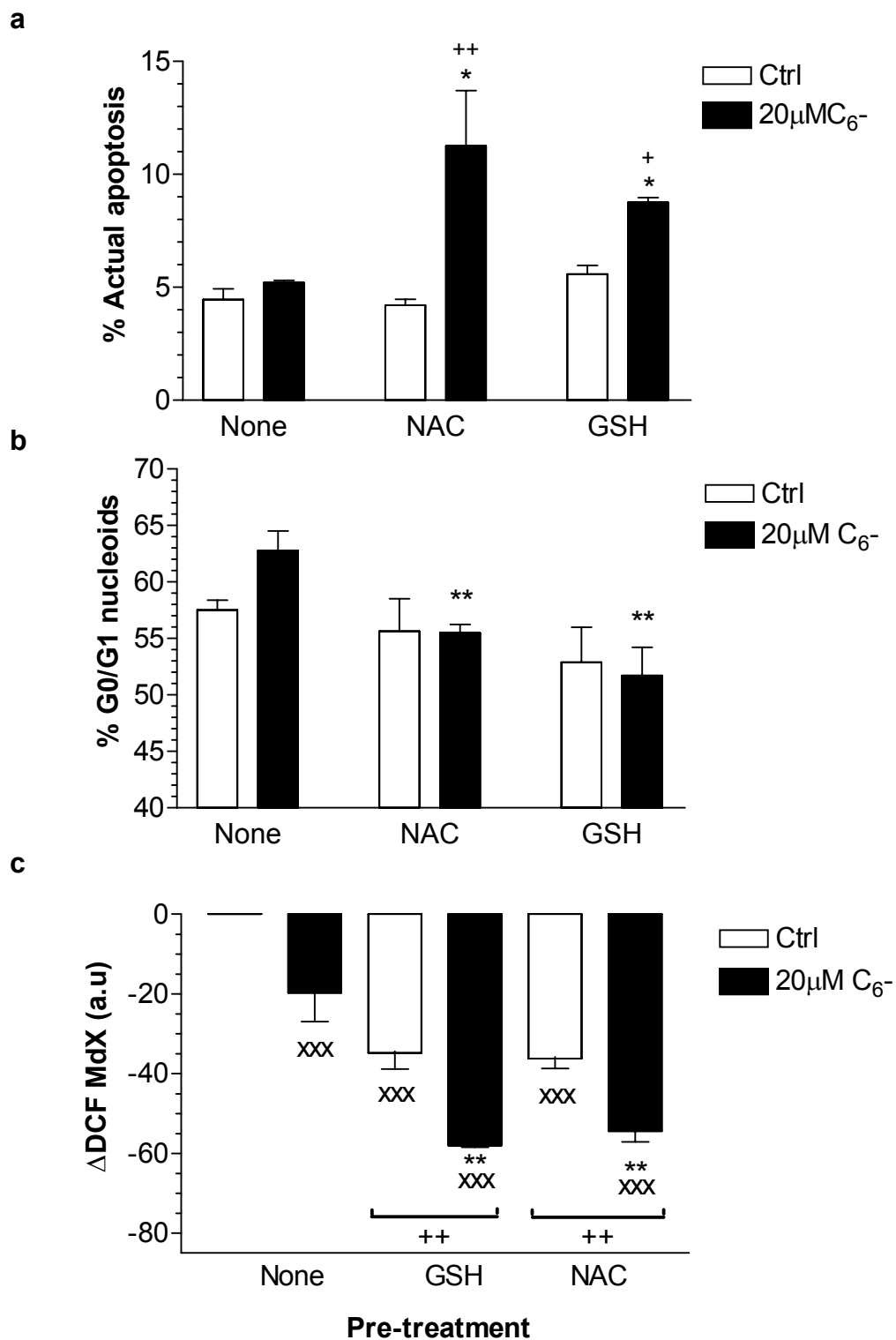


Figure 4.

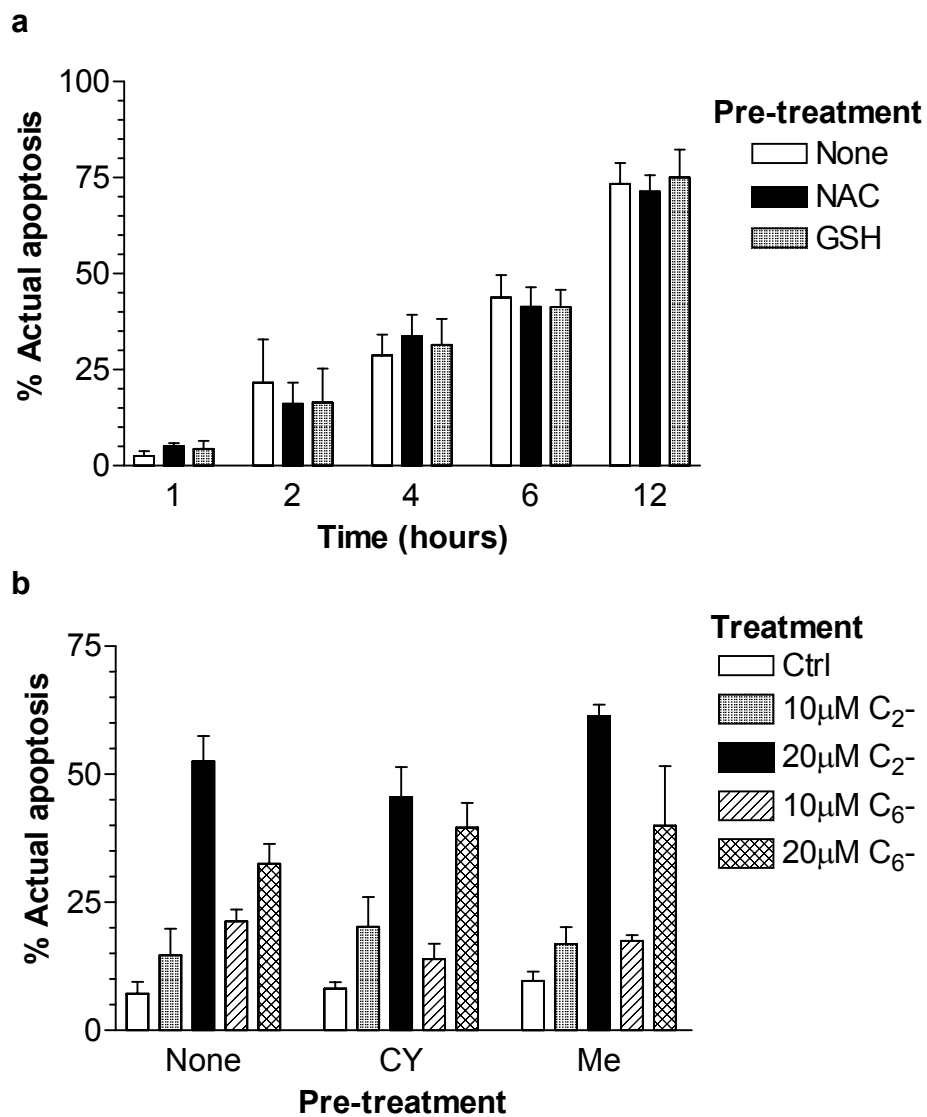


Figure 5.

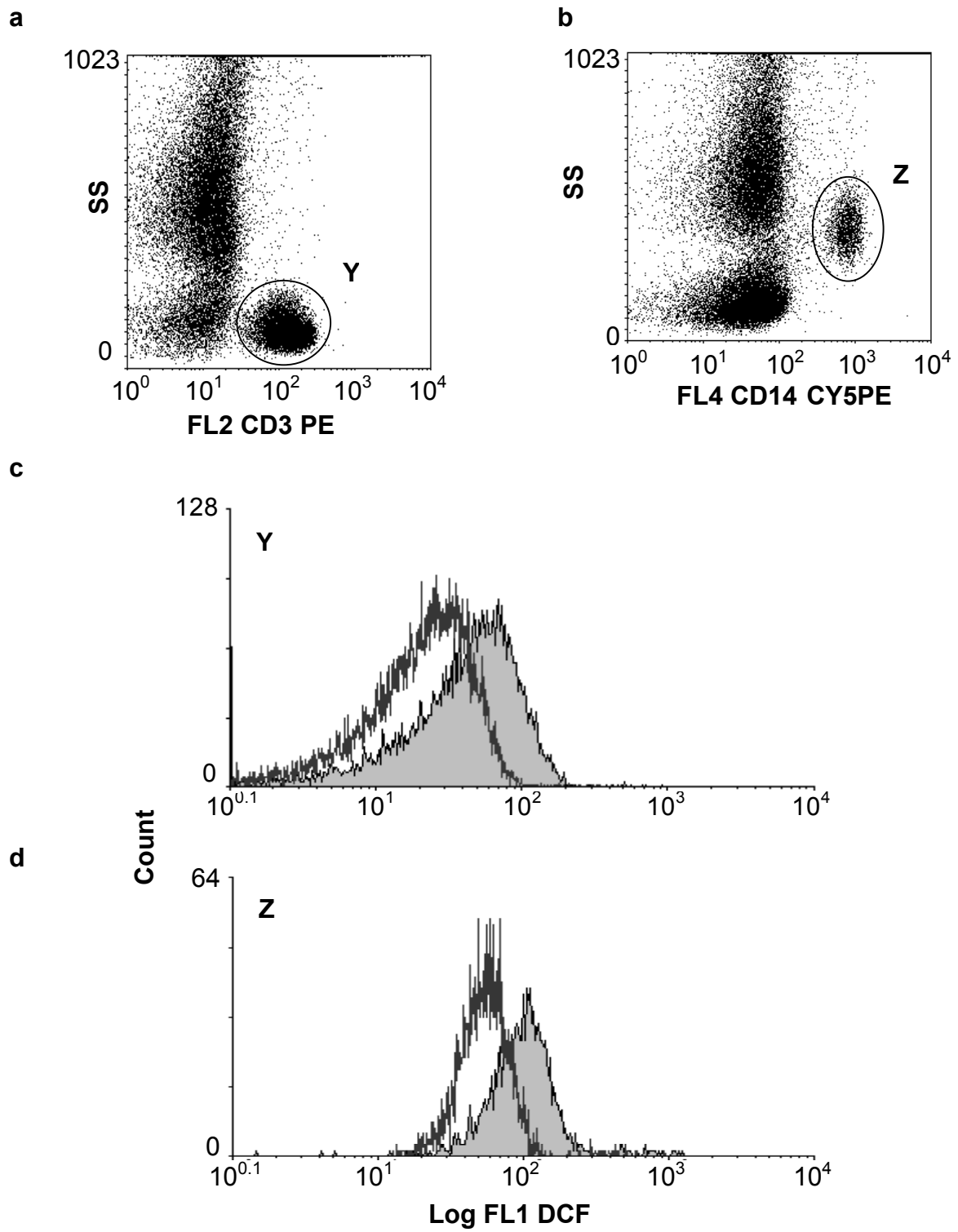
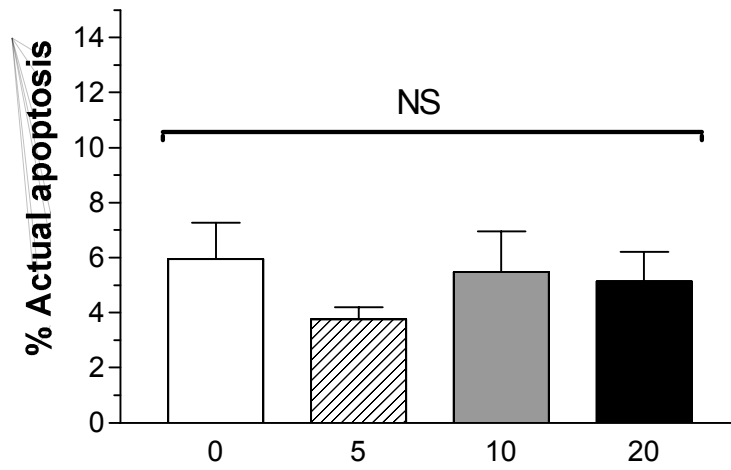
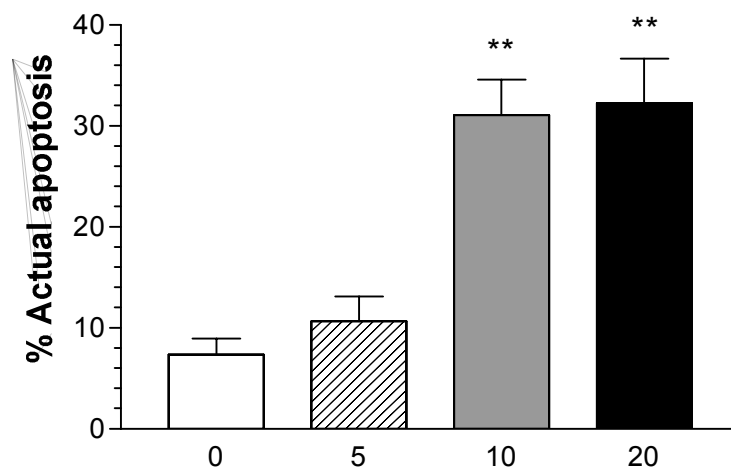


Figure 6.

**a**



**b**



**c**

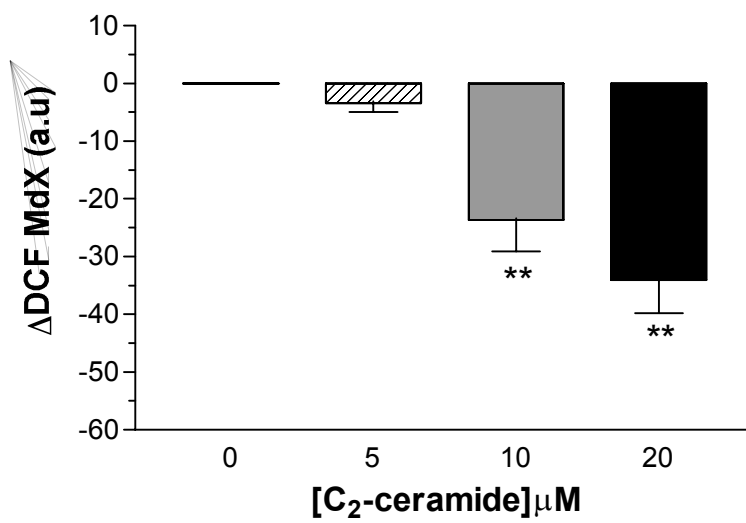


**Figure 7.**

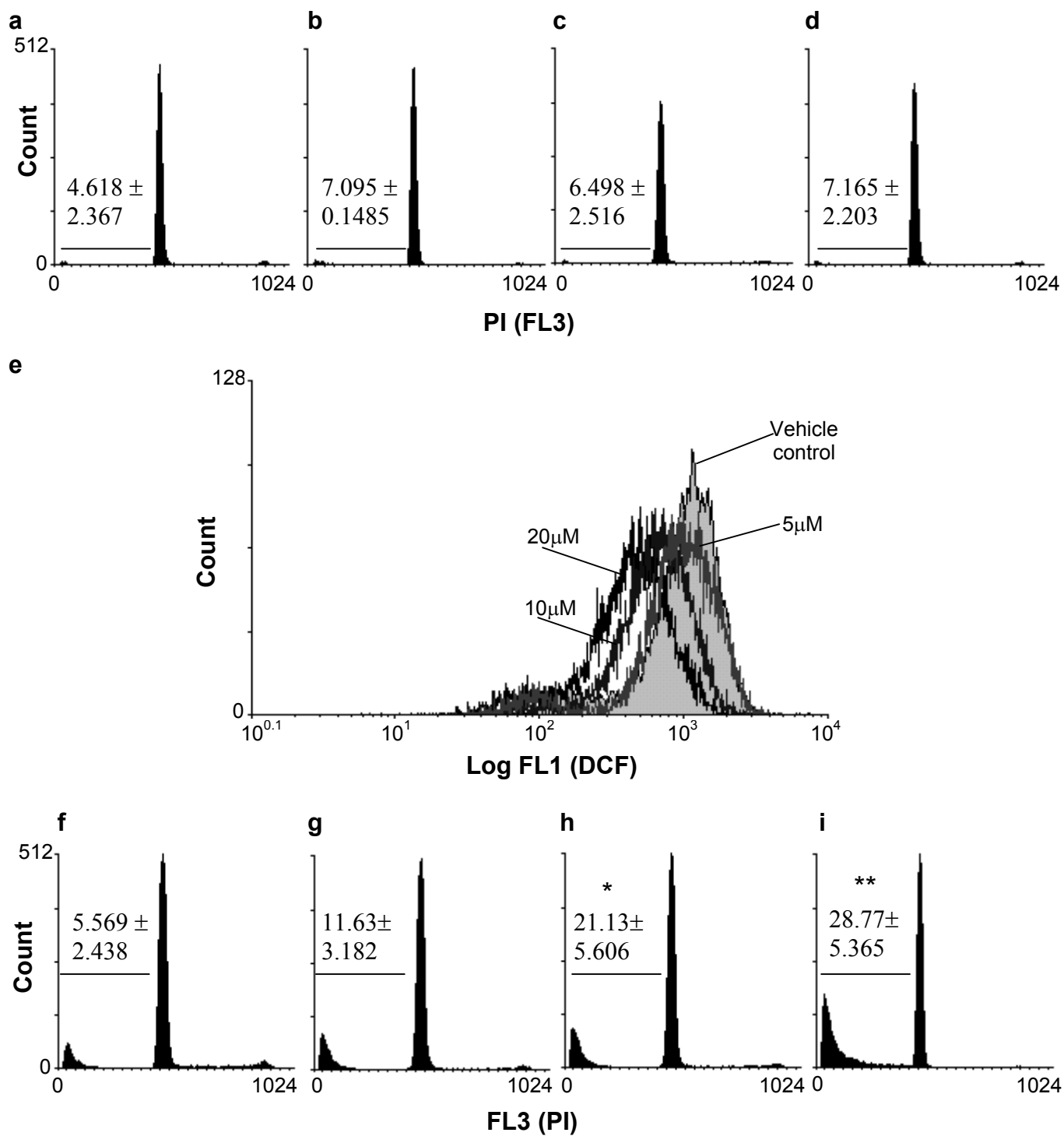


**Figure 8.**

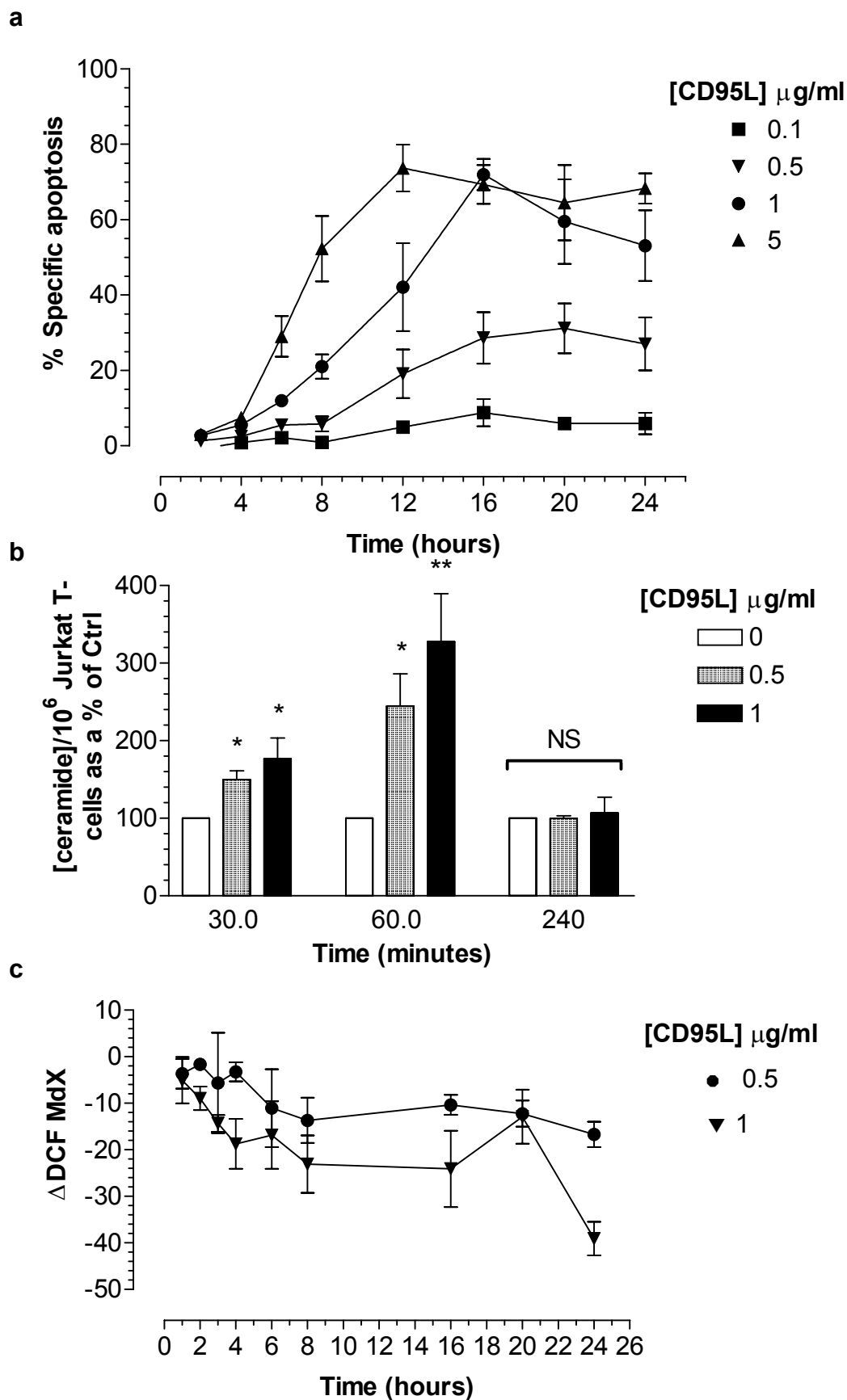


Figure 9.